SPHINGOLIPIDOMICS: QUALIFICATION AND QUANTIFICATION OF SPHINGOLIPIDS IN YEAST

by

Esra Börklü Yücel

B.S. in Ch.E., Boğaziçi University, 2005

Submitted to the Institude for Graduate Studies in
Science and Engineering in partial fulfillment of
the requirements for the degree of
Master of Science

Graduate Program in Chemical Engineering

Boğaziçi University

2005

ACKNOWLEDGEMENTS

I offer my thanks to Prof. Dr. Kutlu Ülgen for her support and counsel throughout this thesis and encouragement she provided during my graduate study.

I would also like to thank Prof. Dr. Betül Kırdar and Prof Dr. Hale Saybaşılı for devoting their precious time to read and comment on my thesis.

This work was financially supported by Boğaziçi Research Fund through project 06S105 and 06A504D and also by TÜBİTAK through project 104M362.

I am sincerely grateful to my friends, Saliha, Betül, Duygu, Dicle, Aylin, Özde, Pınar, Tunahan, Yalçın, Güray and the girls with whom I rowed in the same boat, Ayça and Elif for their continuous support and companionship. I would also thank to my sisters, Pınar, Gaye, Rüveyda and Ergül for their contribution to my life and making it more bearable.

Last, but certainly not the least, I would like to thank to my families for providing me with peace, support, advices and joy throughout my whole life. Most importantly I must express my special thanks to Sinan Yücel, whose contribution to my life is clearly priceless.

ABSTRACT

SPHINGOLIPIDOMICS: QUALIFICATION AND QUANTIFICATION OF SPHINGOLIPIDS IN YEAST

BY4743 parent strain and three homozygous deletion mutants, *ino1Δ/ino1Δ*, *slc1Δ/slc1Δ* and *ser2Δ/ser2Δ*, along with four heterozygous deletion mutants *INO1/ino1Δ*, *SLC1/slc1Δ*, *LCB1/lcb1Δ*, and *LCB2/lcb2Δ* of *S. cerevisiae* are investigated to improve the present knowledge on the synthesis mechanism of sphingolipids in yeast and to qualify as well as to quantify sphingolipid metabolites in *S. cerevisiae* with an ultimate goal of experimental verification of potential drug targets identified by computational methods. Cells were grown in both rich and minimal media in batch cultivations. *ino1Δ/ino1Δ* mutant, aside from these media, was cultivated in minimal medium without inositol. In batch cultivations of YPD, *slc1Δ/slc1Δ* mutant had overgrown the wild type and *ser2Δ/ser2Δ* mutant had the lowest biomass value among all the strains. In F1 medium, both *ino1Δ/ino1Δ* and *slc1Δ/slc1Δ* mutants had overgrown wild type strain while *ino1Δ/ino1Δ* mutant grown in F1 medium without inositol had the lowest biomass value, 1.78 g/l, among all the biomass values of all strains. Optimum lipid extraction procedure was determined by TLC analysis on silica plates. Commercially available mammalian sphingolipid standards as well as phytoceramide and phytosphingosine standards obtained from yeast were analyzed by HPLC to obtain their retention time values and calibration curves. *ser2Δ/ser2Δ* mutant grown in YPD and *ino1Δ/ino1Δ* mutant grown in F1 without inositol media were the strains with noticeable increases in their phytoceramide levels and decreases in biomass values with respect to wild type strain. However, *slc1Δ/slc1Δ* mutant grown in YPD and F1 media had elevated dihydrosphingosine and phytosphingosine levels as well as biomass values compared to wild type strain. Retention time values of 13.175 min and 16.772 min were proposed to be representing the peaks of MIPC and $M(IP)_2C$, respectively, by analyzing HPLC chromatograms of wild type strain grown in YPD and *ino1Δ/ino1Δ* mutant grown in F1 without inositol media.

ÖZET

SİFİNGOLİPİDOMİKS: MAYA SİFİNGOLİPİDLERİNİN TAYİNİ VE MİKTARLARININ BELİRLENMESİ

Hesapsal yöntemlerle belirlenen olası ilaç hedeflerinin deneysel olarak doğrulanması nihai hedefini güden bu çalışmada, *S. cerevisiae*'nın bilinen sifingolipid sentezi mekanizmasının daha iyi anlaşılması, mayanın ürettiği sifingolipid metabolitlerinin tayini ve miktarlarının belirlenmesi amacıyla BY4743 ve bu suştan üç homozigot ve dört heterozigot delesyon suşu olarak yaratılan *ino1Δ/ino1Δ*, *slc1Δ/slc1Δ*, *ser2Δ/ser2Δ*, *INO1/ino1Δ*, *SLC1/slc1Δ*, *LCB1/lcb1Δ*, ve *LCB2/lcb2Δ* suşları incelenmiştir. Bu amaçla, hücreler kesikli üretim ile zengin ve minimal besi ortamlarında büyütülmüş, *ino1Δ/ino1Δ* suşu ayrıca inositol içermeyen besi ortamında da büyütülerek incelenmiştir. Zengin besi ortamında kesikli üretimde *slc1Δ/slc1Δ* suşunun ana suştan daha yüksek miktarlarda hücre ürettiği, *ser2Δ/ser2Δ* suşunun ise zengin ortamda büyüyen tüm suşlar arasında en düşük biyokütle değerine sahip olduğu gözlenmiştir. Minimal besi ortamında, *ino1Δ/ino1Δ* ve *slc1Δ/slc1Δ* suşlarının biyokütle değerleri ana suşunkinden yüksek olup, inositolsüz minimal ortamda büyüyen *ino1Δ/ino1Δ* suşu, tüm suşlardan daha az miktarda hücre üreterek 1.78 g/l lik biyokütle değerine sahip olmuştur. Silika tabakalar kullanılan İTK analizi ile en uygun lipid çekim yöntemi belirlenmiştir. Satın alınan maya (fitosifingozin ve fitoseramid) ve memeli sifingolipid standartları HPLC ile incelenmiş ve kolonda kalma süreleri ile miktar-alan ilişkisine dayanan kalibrasyon eğrileri elde edilmiştir. Yabanıl tip suşla karşılaştırıldıklarında, zengin besi ortamında büyüyen *ser2Δ/ser2Δ* ve inositolsüz minimal besi ortamında büyüyen *ino1Δ/ino1Δ* suşlarında fitoseramid miktarlarında belirgin bir artış ve biyokütle değerlerinde de düşüş gözlemlenmiştir. Ancak zengin ve minimal ortamda büyüyen *slc1Δ/slc1Δ* suşu hem ürettiği hücre miktarı hem de dihidrosifingozin ve fitosifingozin değerleriyle yabanıl tipi geçmiştir. İnositolsüz minimal ortamda büyüyen *ino1Δ/ino1Δ* ve zengin ortamda büyüyen yabanıl tip suşlarının kromatogramları incelenerek kolonda kalma süresi 13.175 dk. ve 16.772 dk. olan bileşenlerin sırasıyla MIPC ve $M(IP)_2C$ oldukları düşünülmektedir.

TABLE OF CONTENTS

ACKNOWLEDGEMENTS iii
ABSTRACT iv
ÖZET v
LIST OF FIGURES ix
LIST OF TABLES xii
LIST OF SYMBOLS/ABBREVIATIONS xv
1. INTRODUCTION 1
2. THEORETICAL BACKGROUND 2
2.1. Structure and Nomenclature of Sphingolipids 2
2.2. Sphingolipid Metabolism in *Saccharomyces cerevisiae* 3
2.3. Functions of Sphingolipids 7
2.3.1. Sphingolipids in Cell Growth and Signalling 8
2.3.2. Sphingolipids in Heat Stress Responses 9
2.3.3. Sphingolipids in Apoptosis 10
2.4. Mutant Strains Used in the Study 11
2.4.1. *INO1* Gene and Its Function 11
2.4.2. *SLC1* Gene and Its Function 12
2.4.3. *SER2* Gene and Its Function 13
2.4.4. *LCB2* and *TSC2(LCB1)* Genes and Their Function 14
3. MATERIALS AND METHODS 15
3.1. Materials 15
3.1.1. Deletion Mutant Strains Adopted 15
3.1.2. Maintenance of the Strains 15
3.1.3. Chemicals and Disposable Materials Used 16
3.1.3.1. Culture Media 16
3.1.3.2. Glassware Required for the Analyses 17
3.1.3.3. Buffers and Chemicals Required for HPLC and TLC Applications 17
3.1.4. Laboratory Equipment 17
3.2. Methods 19

3.2.1. Experimental Methods 19
3.2.1.1. Sterilization 19
3.2.1.2. Cultivation Conditions 19
3.2.1.3. Determination of the Cell Dry Weight 20
3.2.1.4. Lipid Extraction 20
3.2.1.5. Extraction Method Determination by TLC 21
3.2.1.6. HPLC Analysis of the Extracted Lipids 21
4. RESULTS AND DISCUSSION 23
4.1. Growth Characteristics of the Wild Type and Mutant Strains of *S. cerevisiae* 24
4.2. Optimization of Lipid Extraction Procedure by TLC 25
4.3. Detection of Sphingolipid Standards by HPLC 27
4.3.1. C8-Cer 29
4.3.2. C6-Cer 30
4.3.3. C2-Cer 31
4.3.4. P-Cer 32
4.3.5. PHS 33
4.3.6. C18-DHS 34
4.3.7. C20-DHS 35
4.4. Qualificaiton and Quantification of Sphingolipids of *S. cerevisiae* Strains 36
4.4.1. Peak Annotation and Determination for Yeast Sphingolipids 37
4.4.2. Sphingolipid Qualification and Quantification for BY4743 41
4.4.3. Sphingolipid Qualification and Quantification for *INO1* 44
4.4.4. Sphingolipid Qualification and Quantification for *SLC1* 51
4.4.5. Sphingolipid Qualification and Quantification for *SER2* 55
4.4.6. Sphingolipid Qualification and Quantification for *LCB1* and *LCB2* 58
5. CONCLUSIONS AND RECOMMENDATIONS 63
5.1. Conclusions 63
5.2. Recommendations 65
APPENDIX A: CALIBRATION CURVES 67
A.1. Calibration Curve and Equation for C8-Cer 67
A.2. Calibration Curve and Equation for C6-Cer 67
A.3. Calibration Curve and Equation for C2-Cer 68
A.4. Calibration Curve and Equation for P-Cer 69

A.5. Calibration Curve and Equation for PHS 69
A.6. Calibration Curve and Equation for C18-DHS 70
A.7. Calibration Curve and Equation for C20-DHS 71
REFERENCES 72

LIST OF FIGURES

Figure 2.1. Sphingolipid pathway in yeast 4

Figure 2.2. Some of the yeast sphingolipids 8

Figure 4.1. Acetone activated TLC results with procedure #1 extraction 25

Figure 4.2. Acetone activated TLC results with procedure #2 extraction 26

Figure 4.3. Heat activated TLC results with procedure #1 extraction 26

Figure 4.4. Heat activated TLC results with procedure #2 extraction 27

Figure 4.5. Autoscaled chromatogram of C8-Cer 29

Figure 4.6. Autoscaled chromatogram of C6-Cer 30

Figure 4.7. Autoscaled chromatogram of C2-Cer 31

Figure 4.8. Autoscaled chromatogram of P-Cer 32

Figure 4.9. Autoscaled chromatogram of PHS 33

Figure 4.10. Autoscaled chromatogram of C18-DHS 34

Figure 4.11. Autoscaled chromatogram of C20-DHS 35

Figure 4.12. Structures of ceramides (a) inositol-phosphorylceramide and (b) C8-Cer. 38

Figure 4.13. Structures of sphingolipids (a) DHS-P and (b) C2-Cer 39

Figure 4.14. Chromatogram of BY743 grown in YPD..... 41

Figure 4.15. Chromatogram of BY743 grown in F1 42

Figure 4.18. Chromatogram of *ino1Δ/ino1Δ* mutant grown in YPD..... 44

Figure 4.19. Chromatogram of *INO1/ino1Δ* mutant grown in YPD 45

Figure 4.20. Chromatogram of *ino1Δ/ino1Δ* mutant grown in F1 45

Figure 4.21. Chromatogram of *ino1Δ/ino1Δ* mutant grown in F1 without inositol..... 46

Figure 4.22. TLC analysis of wild type and mutant strains sphingolipids..... 47

Figure 4.23. Chromatogram of *SLC1/slc1Δ* mutant grown in YPD..... 51

Figure 4.24. Chromatogram of *slc1Δ/slc1Δ* mutant grown in YPD..... 52

Figure 4.25. Chromatogram of *slc1Δ/slc1Δ* mutant grown in F1..... 52

Figure 4.26. Chromatogram of *ser2Δ/ser2Δ* mutant grown in YPD..... 57

Figure 4.27. Chromatogram of *LCB1/lcb1Δ* mutant grown in YPD..... 58

Figure 4.28. Chromatogram of *LCB2/lcb2Δ* mutant grown in YPD..... 59

Figure A.1. Calibration curve for C8-Cer..... 67

Figure A.2. Calibration curve for C6-Cer..... 68

Figure A.3. Calibration curve for C2-Cer..... 68

Figure A.4. Calibration curve for P-Cer 69

Figure A.5. Calibration curve for PHS 70

Figure A.6. Calibration curve for C18-DHS 70

Figure A.7. Calibration curve for C20-DHS 71

LIST OF TABLES

Table 2.1. Sphingolipid classes and subclasses 3

Table 3.1. Parameters of the HPLC system 22

Table 4.1. Biomass (g/l) values of strains grown in different media 25

Table 4.2. Functions and properties of sphingolipid standards..... 28

Table 4.3. Injection results of C8-Cer 30

Table 4.4. Injection results of C6-Cer 31

Table 4.5. Injection results of C2-Cer 32

Table 4.6. Injection results of P-Cer..... 33

Table 4.7. Injection results of PHS..... 34

Table 4.8. Injection results of C18-DHS 35

Table 4.9. Injection results of C20-DHS 36

Table 4.10. Sphingolipid concentrations for BY4743 at steady-state..... 37

Table 4.11. Peak results for BY4743 grown in YPD 38

Table 4.12. Peak results for *ino1Δ/ino1Δ* grown in F1 39

Table 4.13. Sphingolipid profile of BY4743 grown in YPD..... 40

Table 4.14. Comparison of experimental data with literature for BY4743 grown in YPD 41

Table 4.15. Summary of sphingolipid profiles of BY4743 grown in YPD 42

Table 4.16. Summary of sphingolipid profiles of BY4743 grown in F1 43

Table 4.17. Comparison of experimental data with literature for BY4743 grown in F1 44

Table 4.18. Summary of sphingolipids of *ino1Δ/ino1Δ* mutant grown in YPD 46

Table 4.19. Summary of sphingolipids of *ino1Δ/ino1Δ* mutant grown in F1 without inositol 47

Table 4.20. Summary of sphingolipids of *INO1/ino1Δ* mutant grown in YPD 48

Table 4.21. Summary of sphingolipids of *ino1Δ/ino1Δ* mutant grown in F1 49

Table 4.22. Comparison of experimental data of *ino1Δ/ino1Δ* mutant in YPD with that of BY4743 49

Table 4.23. Comparison of experimental data of *INO1/ino1Δ* mutant in YPD with that of BY4743 50

Table 4.24. Comparison of experimental data of *ino1Δ/ino1Δ* mutant in F1 without inositol with that of BY4743 in F1 50

Table 4.25. Comparison of experimental data of *ino1Δ/ino1Δ* mutant in F1 with data of BY4743 in F1 50

Table 4.26. Summary of sphingolipids of *slc1Δ/slc1Δ* mutant grown in F1 53

Table 4.27. Comparison of experimental data of *slc1Δ/slc1Δ* mutant in F1 with data for BY4743 in F1 53

Table 4.28. Summary of sphingolipids of *slc1Δ/slc1Δ* mutant grown in YPD 54

Table 4.29. Comparison of experimental data of *slc1Δ/slc1Δ* mutant in YPD with that of BY4743 in YPD..... 54

Table 4.30. Summary of sphingolipids of *SLC1/slc1Δ* mutant grown in YPD 55

Table 4.31. Comparison of experimental data of *SLC1/slc1Δ* mutant in YPD with that of BY4743 in YPD..... 55

Table 4.32. Summary of sphingolipids of *ser2Δ/ser2Δ* mutant grown in YPD..... 56

Table 4.33. Comparison of experimental data of *ser2Δ/ser2Δ* mutant in YPD with that of BY4743 in YPD..... 58

Table 4.34. Summary of sphingolipids of *LCB2/lcb2Δ* mutant grown in YPD 59

Table 4.35. Summary of sphingolipids of *LCB1/lcb1Δ* mutant grown in YPD 60

Table 4.36. Comparison of experimental data of *LCB1/lcb1Δ* mutant in YPD with that of BY4743 in YPD..... 61

Table 4.37. Comparison of experimental data of *LCB2/lcb2Δ* mutant in YPD with that of BY4743 in YPD..... 61

Table 5.1. Summary of sphingolipid proportions of different strains..... 65

LIST OF SYMBOLS / ABBREVIATIONS

R^2	Correlation indice
C2-Cer	Acetyl ceramide
C6-Cer	Caproyl ceramide
C8-Cer	N-Octanoyl-D- sphingosine
C18-DHS	N-Stearoyl-D-*erythro*-Sphinganine
C20-DHS	D-*erythro*-Sphinganine (C20)
DAG	Diacylglycerol
D-Cer	Dihydroceramide
DHS	Dihydrosphingosine
DHS-P	Dihydrosphingosine-1-phosphate
ELSD	Evaporative light scattering detector
ERK	Extracellular signal regulated kinase
Fas-L	Fas ligand
HPLC	High performance liquid chromatography
IPC	Inositol phosphoryl ceramide
JNK	Jun-N-terminal kinases
LCB	Long chain base
MAPK	Mitogen activated protein kinase
MCA	Metabolic control analysis
MIPC	Mannosyl inositol phosphoryl ceramide
$M(IP)_2C$	Mannosyl diinositol phosphoryl ceramide
MKK / MEK	MAPK kinase
NGF	Nerve growth factor
PA	Phosphatidic acid
P-Cer	Phytoceramide
PHS	Phytosphingosine
PHS-P	Phytosphingosine-1-phosphate
PI	Phosphadityl inositol

PS	Phosphadityl serine
RNA	Ribonucleic acid
rpm	Rotations per minute
SPT	Serine palmytoyl transferase
TBP	TATA binding protein
TLC	Thin layer chromatography
TNFα	Tumor necrosis factor alpha
v/v	Volume per volume
w/v	Weight per volume
YPD	Yeast extract- peptone-dextrose

1. INTRODUCTION

It has been more than 120 years since sphingolipids were first described in biological systems as essential building blocks of the plasma membranes of all eukaryotic cells and some prokaryotic organisms or viruses. Today, sphingolipids have been determined to be highly bioactive in the regulation of diverse cellular functions.

The attention of researchers focused on sphingolipids after discovery of the inhibition of protein kinase C (PKC) by sphingoid bases in 1986 (Hannun *et al.*, 1986, Merrill *et al.*, 1986). Next, it was found that sphingomyelin could be hydrolyzed and the ceramide levels could be increased independent of protein kinase C (Kolesnick, 1987). The hypothesis, that sphingolipid-derived metabolites could function as second messengers, was confirmed later through a better understanding of the sphingomyelin pathway, the physiological functions of ceramide, and the regulation of cell proliferation and apoptosis (Spiegel *et al.*, 1996). As for many bioactive lipids in general, sphingolipid signaling mechanisms often involve specific protein-lipid interactions through specific domains.

In the study of sphingolipids, *Saccharomyces cerevisiae* was usually highlighted because more was known about its sphingolipids and it was very likely to be the first eucaryotic organism for which all genes necessary for sphingolipid metabolism were identified. Making use of the knowledge about these genes, researchers would have a higher chance to biochemically characterize sphingolipid metabolic enzymes, and to identify and characterize new functions for sphingolipids (Obeid *et al.*, 2002).

The Theoretical Background section of this work included basic information on the structure of sphingolipids, sphingolipid metabolism in *Saccharomyces cerevisiae*, mutant strains used in the study along with functions of sphingolipids in the cell. In Materials and Methods section, the procedures followed in the experiments as well as the chemicals used were given. Results and Discussion part comprised of the results obtained along with the comments on sphingolipid profiles of different strains used in the present work. Finally, conclusions and recommendations to improve the quality of the results were given in Chapter 5.

2. THEORETICAL BACKGROUND

The family of compounds termed sphingolipids is one of the most complex and structurally diverse lipids due to the large number of possible combinations of hydrophobic backbones and headgroups. Sphingolipids are highly bioactive compounds that serve not only as components of biologic structures such as membranes and lipoproteins, but also as regulators of cell proliferation, differentiation, cell–cell and cell–matrix interactions, cell migration, intracellular (and extracellular) signaling, membrane tracking, autophagy, and cell death (Merril *et al.*, 2005).

For most of these functions, there is structural specificity with respect to the major sphingolipid subclass (for example, in many cases ceramides are growth inhibitory whereas sphingoid base 1-phosphates usually stimulate growth), and within subclass, changes as minor as the presence or absence of a double bond can have a major impact on function.

2.1. Structure and Nomenclature of Sphingolipids

Sphingolipids are composed of a sphingoid base backbone that is synthesized de novo from serine and a long-chain fatty acyl-CoA, then converted into ceramides, phosphosphingolipids, glycosphingolipids, and other species, including protein adducts (Fahy *et al.*, 2005). A number of organisms also produce sphingoid base analogs that have many of the same features as sphingolipids (such as long-chain alkyl and vicinal amino and hydroxyl groups) but differ in other features.

Sphingolipids can be divided into several major classes: the sphingoid bases and their simple derivatives (such as the 1-phosphate), the sphingoid bases with an amide-linked fatty acid (e.g., ceramides), and more complex sphingolipids with head groups that are attached via phosphodiester linkages (the phosphosphingolipids), via glycosidic bonds (the simple and complex glycosphingolipids), and other groups (Fahy *et al.*, 2005). The IUPAC has recommended a systematic nomenclature for sphingolipids.

Table 2.1. Sphingolipid classes and subclasses (Fahy *et al.*, 2005)

Sphingoid bases	**Ceramides**	**Phospho sphingolipids**	**Neutral glyco sphingolipids**	**Acidic glyco sphingolipids**
Sphing-4-enines (sphingosines)	N-Acylsphingosines (ceramides)	Ceramide phosphocholines (sphingomyelins)	Simple Glc series (GlcCer, LacCer, etc.)	Gangliosides
Sphinganines	N-Acylsphinganines (dihydroceramides)	Ceramide phospho ethanolamines	globo series	Sulfoglyco sphingolipids (sulfatides)
phytosphingosines	N-Acyl-4-hydroxysphinganines (phytoceramides)	Ceramide phosphoinositols	ganglio series	Glucurono sphingolipids
Sphingoid base homologs and variants	Acylceramides		lacto series	Phosphoglyco sphingolipids
Sphingoid base 1-phosphates	Ceramide 1-phosphates		neolacto series	

2.2. Sphingolipid Metabolism in *Saccharomyces cerevisiae*

It has become increasingly evident that sphingolipids, once thought to be only structural components of cell membranes, are now known to be important molecules in cell regulation. They have important roles in cell stress responses whereby they mediate diverse biological responses such as cell growth, apoptosis, angiogenesis, differentiation, and senescence. To understand how sphingolipids regulate these important cellular processes, it is necessary to understand how sphingolipids are regulated. So deciphering and dissecting sphingolipid metabolism is critical to gaining insight into cell regulation.

Steps in *Saccharomyces cerevisiae* sphingolipid metabolism are outlined in Figure 2.1. (Alvarez-Vasquez *et al.*, 2005). Sphingolipid synthesis begins with the condensation of palmitoyl- CoA and serine to yield 3-ketodihydrosphingosine (3-ketosphinganine) by Tsc2p (Lcb1p) and Lcb2p, which is reduced to yield DHS. In *Saccharomyces cerevisiae*

DHS is rapidly amide-linked to a C-26 fatty acid to give N-acylsphinganine (Dihydro-C in Figure 2.1). Dihydroceramide (Ceramide-1 in Figure 2.1) is hydroxylated at C-4 by Sur2p/Syr2p to give phytoceramide (Ceramide-2 in Figure 2.1). Alternatively, DHS is hydroxylated at C-4 by Sur2p/Syr2p to give PHS, which is acylated to give ceramide-2. In mammals, DHS is acylated, usually with a C-18 fatty acid, and the resulting dihydroceramide then serves as a substrate for formation of the 4,5- trans double bond found in the sphingosine component of ceramides (Dickson and Lester, 1999a).

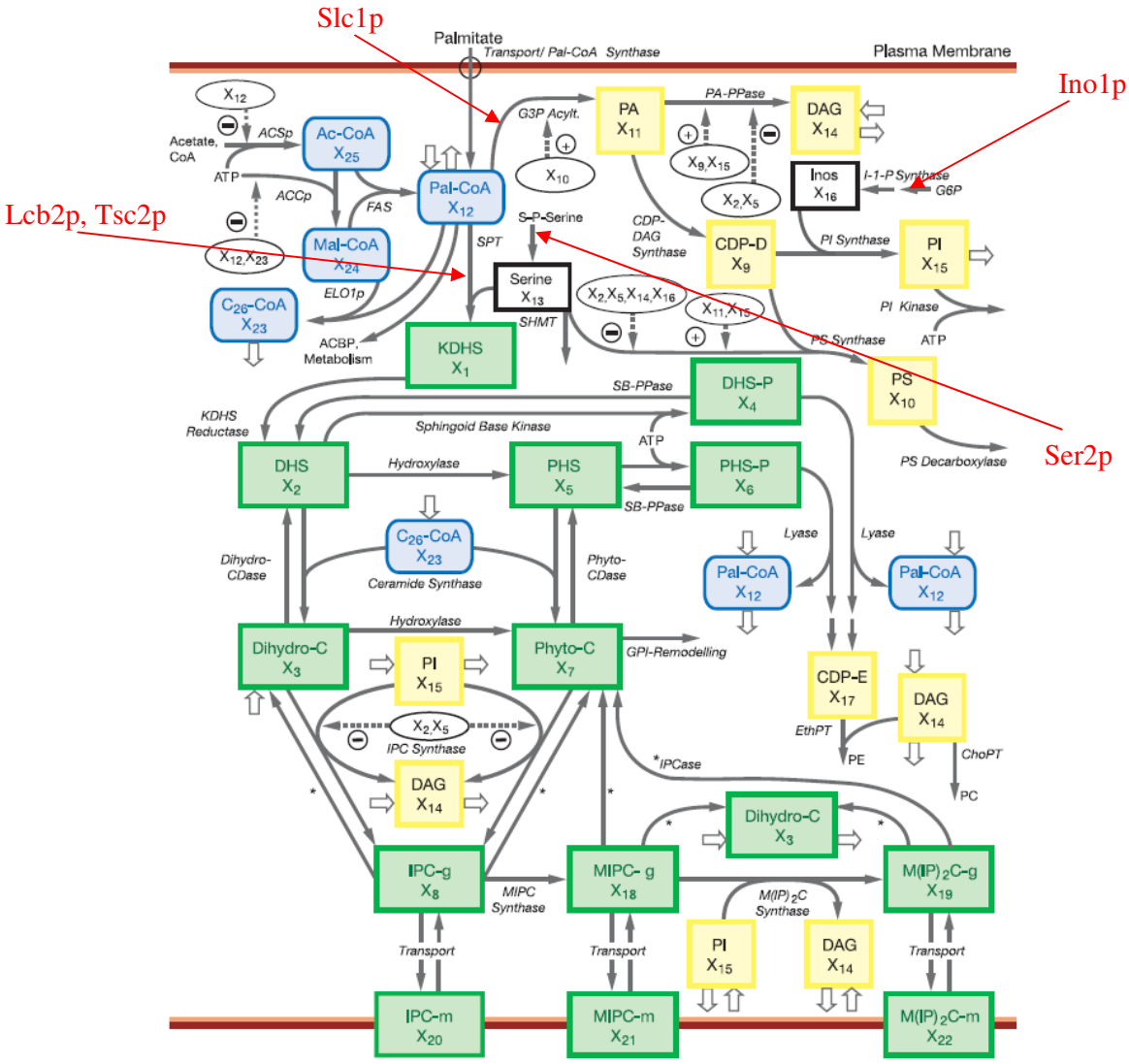

Figure 2.1. Sphingolipid pathway in yeast (Alvarez-Vasquez *et al.*, 2005)

Saccharomyces cerevisiae, most other fungi, and plants make sphingolipids that contain myo-inositol. The three myo-inositol-containing sphingolipids in *Saccharomyces cerevisiae*, as can be seen in Figure 2.1, are inositol-phosphoceramide (IPC), mannose-inositol-phosphoceramide (MIPC) and mannose-(inositol-P) 2-ceramide (MIP_2C). The structure of these compounds is incomplete. Available data indicate that the phosphorus in IPC is linked to the 1-OH of ceramide and inositol. NMR spectroscopy of the complete head group of $M(IP)_2C$ suggest that the structure of $M(IP)_2C$ is inositol-1-P(6)mannose (K-1,2) inositol-1-P-(1)ceramide (Smith and Lester, 1974). Addition of inositol phosphate is the only known modification to the C-1 OH of ceramides in *Saccharomyces cerevisiae*. It is possible that other unidentified modifications are made, but they could only be present in small amounts (Dickson and Lester, 1999b). In addition, some fungi and all plant species that have been examined add one or more sugar residues to the C-1 of ceramide to form a second class of sphingolipids referred to as glycosylceramides. Animals do not add inositol phosphate to ceramide, but instead they add phosphocholine to form sphingomyelin or glucose or galactose that can be further decorated with carbohydrates and sometime with sulfates to form hundreds of complex sphingolipids (Merrill and Sweeley, 1996). Once it became clear that sphingolipid synthesis is essential for the viability of *Saccharomyces cerevisiae* cells and that IPC is not made by animals, it was logical to infer that inhibitors of IPC synthase (phosphatidylinositol:ceramide phosphoinositol transferase) might be effective anti-fungal drugs. A major impetus for using IPC synthase as a target for anti-fungal drugs was the discovery that aureobasidin A, is a potent inhibitor of IPC synthase activity and that the AUR1 gene encodes IPC synthase or is a subunit of the enzyme (Nagiec *et al.*, 1997).

It is assumed that the synthesis of sphingolipids begins in the endoplasmic reticulum and proceeds up to formation of ceramide or IPC. This assumption is based primarily upon work done in mammals (Nagiec *et al.*, 1997). With three exceptions, there is no direct evidence in *Saccharomyces cerevisiae*, contrary to what is stated in various publications and databases, that the enzymes necessary for ceramide synthesis are located in the endoplasmic reticulum. The three exceptions are Csg2p, Fen1(Elo2)p and Sur4(Elo3)p which were found to be localized in the endoplasmic reticulum by light microscopy techniques (David *et al.*, 1998). Fen1p and Sur4p are necessary for elongation of C-22 fatty acids to C-26. The enzymes acting on ceramides to form IPC, MIPC or $M(IP)_2C$ and

the enzymes for metabolism of DHS-1-phosphate or PHS-1-phosphate (Figure 2.1) have not been localized to specific cellular compartments in *Saccharomyces cerevisiae* (Dickson and Lester, 1999a). Synthesis of some species of IPC and their conversion to MIPC and MIP_2C is thought to occur in the Golgi apparatus based upon their intracellular accumulation in mutants blocked at specific steps in the protein secretory pathway (Puoti *et al.*, 1991).

$M(IP)_2C$ accounts for about seventy five per cent of the mass of total sphingolipids with the remainder being equally divided between IPC and MIPC. It is estimated that these three sphingolipids make up seven-eight per cent of the mass of the plasma membrane since they constitute thirty per cent of the plasma membrane phospholipids. Because of their large mass and large negative charge they likely have general effects on processes that are dependent upon the plasma membrane (Dickson and Lester, 1999a).

Breakdown of membrane sphingolipids is essential in mammals and occurs both as a part of normal cellular metabolism and in the generation of sphingolipid second messengers (Merrill *et al.*, 1996). In *Saccharomyces cerevisiae*, it has been detected that one or more phospholipase C-like activities in cell-free extracts release ceramide and the polar head groups from sphingolipids. In addition, yeast extracts have been shown to contain an enzyme that releases ceramide from sphingomyelin. The identity of these phospholipase activities awaits determination, as does their physiological function (Dickson and Lester, 1999a).

It was assumed that long-chain bases including 3-keto-DHS, DHS and PHS were taken up from the culture medium and used directly as substrates by the appropriate enzyme in the biosynthetic pathway shown in Figure 2.1. Available evidence now indicates that this assumption is wrong and that at least DHS and PHS must first be phosphorylated and then dephosphorylated in order to be incorporated in sphingolipids. The first hint of this pathway came from studies of mutants that failed to incorporate [^{3}H]DHS into sphingolipids (Dickson and Lester, 1999a). These studies uncovered a gene, termed LCB3, which was required for incorporation of exogenous [^{3}H]DHS into sphingolipids (Qie *et al.*, 1997). Soon thereafter, LCB3 was identified as a phosphatase that could dephosphorylate DHS-1-P and PHS-1-P (Dickson and Lester , 1999a).

2.3. Functions of Sphingolipids

Sphingolipids are abundant components of the *Saccharomyces cerevisiae* plasma membrane, with smaller amounts found in other cellular membranes. Despite their abundance, functional roles in cellular processes have only begun to be elucidated in the past decade. Interest in sphingolipids has been sparked by indications that they regulate signal transduction pathways in mammals (Merrill *et al.*, 2005).

Whether or not sphingolipids are signaling molecules or second messengers in *Saccharomyces cerevisiae* remains to be established, but recent data, to be discussed here, suggest that they are playing such a role during heat stress (Obeid *et al.*, 2002). They may also be second messengers during osmotic and low pH stress (Kihara and Igarashi, 2004). Functions of sphingolipids include facilitating transport of glycosyl phosphatidylinositol-anchored proteins from the endoplasmic reticulum to the Golgi apparatus, being the lipid moiety in many glycosylphosphatidylinositol- anchored proteins, playing some role in regulating calcium homeostasis or being components in calcium- mediated signaling pathways, and regulating the cell cycle. Interest in sphingolipids increased by the suggestion that ceramide, the basic building block of sphingolipids, is a signaling molecule in mammals formed by hydrolysis of sphingomyelin in response to binding of a ligand to an extracellular membrane receptor (Kolesnick, 1987).

Erectors of ceramide production include Fas ligands, ultraviolet light, heat shock, DNA damage, chemotherapeutic drugs and many other agents. The activated signal transduction pathways control a variety of cellular processes including the cell cycle, apoptosis and senescence, immune responses, and cell-cell interactions (Colombaionia and Gil, 2004). Ceramide is one of many intermediates in sphingolipid metabolism and it seemed likely that other sphingolipid metabolites might function as signaling molecules. Subsequently, it has been shown that sphingosine, as can be seen in Figure 2.2 and sphingosine-1-phosphate, sphingosylphosphorylcholine, and possibly di and tri-N-methylsphingosine are signaling molecules that regulate numerous cellular processes in mammals (Reynolds *et al.*, 2004).

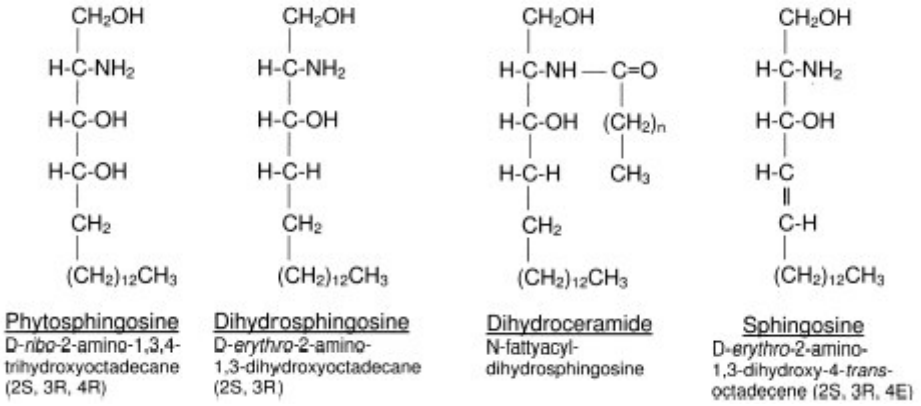

Figure 2.2. Some of the yeast sphingolipids (Dickson and Lester,1999)

Sphingolipids in yeast have been shown to mediate significant and diverse biologic responses. Insight from these studies can also be translated to mammalian cell regulation.

2.3.1. Sphingolipids in Cell Growth and Signalling

Sphingolipids are essential for yeast cell growth and survival based on the observation that inactivation of biosynthesis of sphingolipids leads to lethality of yeast cells. Yeast cells with a mutation in either LCB1 or LCB2 are inviable unless an exogenous LCB (DHS or PHS) is supplied (Dickson and Lester, 1999). Fumonisin B1, a ceramide synthase inhibitor that inhibits both biosynthesis of ceramides and of complex sphingolipids, also inhibits yeast growth. Yeast cells with the deletion of IPC synthase fail to synthesize complex sphingolipids and die. These studies suggest that complex sphingolipids are essential for yeast survival and growth. On the other hand, some of the intermediates of sphingolipids such as ceramide, LCBs, and LCBPs have an inhibitory effect on yeast growth. Also, the fact that C2-ceramide inhibited yeast cell growth at the micromolar range is observed (Fishbein *et al.*, 1993). Further, it was shown that C2-ceramide inhibited proliferation of yeast cells by arresting them at the G1 phase of the cell cycle, and that this cell cycle arrest was through activation of the yeast ceramide-activated protein phosphatase (CAPP) (Nickels and Broach, 1996). It was later shown that exogenous sphingosine and phytosphingosine also induced growth inhibition of yeast cells. It is possible that the lethality of the *IPC1* deletion mutant is a result of accumulation of ceramides and sphingoid bases (Chung *et al.*, 2001).

2.3.2. Sphingolipids in Heat Stress Responses

The protective role of sphingolipids in cell growth and survival under heat stress conditions was first speculated based on the observation that a yeast mutant *SLC1* lacking the ability to synthesize sphingolipids is unable to grow at an elevated temperature. (>37 °C) (Dickson *et al.*, 1990). Because ceramides, sphingoid bases, and their phosphates are increased in response to heat stress and they are metabolically interchangeable in yeast cells, it is still unknown whether one or all of these lipids has a protective effect against heat stress and heat shock. With the cloning of most enzymes responsible for metabolism of sphingolipids, it is possible to address this issue by constructing yeast mutants that generate one but not the other lipids (Obeid *et al.*, 2002).

The pathways for the generation of sphingoid bases, ceramide, and sphingoid base phosphates upon heat stress have not been well defined. It was initially thought that ceramides, sphingoid bases and their phosphates were generated only *de novo* in response to heat stres (Wells *et al.*, 1998). However, identification of enzymes responsible for breakdown of complex sphingolipids and ceramides raises the possibility that ceramides, sphingoid bases and their phosphates can also be generated from breakdown of sphingolipids. But still, the increased ceramide in response to heat stress appears to come from *de novo* biosynthesis because australifungin, the specific inhibitor for ceramide synthase, is able to block most of the increase in ceramide induced by heat stress. It was speculated that DHS is only generated *de novo* because breakdown of complex sphingolipids, which do not contain the DHS moiety, cannot generate DHS. However, a recent identification of a yeast dihydroceramidase suggests that DHS can also be generated from hydrolysis of dihydroceramide (Wells *et al.*, 1998).

After the original observation that heat increased sphingoid base production through SPT and the finding that the increase could be selectively blocked with a heat-sensitive allele for LCB1, a requirement for *de novo* sphingoid bases for the arrest is demonstrated (Jenkins and Hannun, 2001). Whereas parental strains arrest by one hour of heat stress and then resume the cell cycle by two hours, lcb1-100 cells failed to arrest and subsequently died. This finding emphasizes the importance of sphingolipids in stress responses. Interestingly, whereas the lcb4/5 double deletion strain, which accumulates high levels of

sphingoid bases, showed a normal heat-induced arrest, it failed to re-enter the cell cycle, which prompted the speculation that degradation of bases via their conversion to phosphorylated derivatives was required to permit continuation of the cell cycle (Jenkins and Hannun, 2001). It is uncertain how these studies relate to those described above wherein buildup of sphingoid base phosphates inhibited cell cycle progression. Thus, further study is required to dissect respective roles of sphingoid bases vs. their phosphates in the regulation of cell cycle progression.

2.3.3. Sphingolipids in Apoptosis

Ceramide (N-Acyl-Sphingosine) is the precursor of sphingophospholipids which are part of the cell membrane. Naturally occurring ceramides consist of a long-chain sphingoid base with an amid-linked fatty acid substituent (typically 16-24 carbon atoms long). There is evidence that the generation of ceramide by hydrolysis of sphingophospholipids (e.g. sphingomyelin) is associated with the induction of apoptotic cell death. Ceramide is generated in cells as a result of three distinct enzymes: neutral and acidic sphingomyelinase (N-SMase and A-SMase) and ceramide synthase (Colombaionia and Gil, 2004).

Ceramide has been involved in apoptosis, differentiation or survival. The effect of ceramide might depend on cell type, on developmental stage of the cell, on type of stimulus and on pathway and amount of ceramide generation. Usually low doses of ceramide result in protection while higher doses induce apoptosis in cultured cells (Irie and Hirabayashi, 1998).

The mechanism by which ceramide mediates its apoptotic effect is not known. It was reported that ceramide can induce apoptotic events in (membrane- and mitochondria-free) cytoplasmic extracts from untreated cells in a cell free system but now it appears that ceramide itself does not trigger apoptosis but relies on the presence of membranes and/or mitochondria. The subcellular localization of ceramide generation can be relevant for its effect. By transfecting SMases directed to different subcellular localizations, it is recently demonstrated that only increases in mitochondrial ceramide result in apoptosis in non-neural cells (Birbes *et al.*, 2001). In some systems ceramide might mediate its apoptotic

effect in combination with its metabolites, the sphingoid bases sphingosine and dihydrosphingosine (= sphinganine) (Colombaionia and Gil, 2004).

Ceramide is implicated in both intrinsic and extrinsic pathways of cell death; it has been involved in apoptosis activated by death domain receptor ligands such as Fas-L and TNFα, NGF, irradiation, hypoxia, serum withdrawal and anticancer drugs. (Colombaionia and Gil, 2004). The apoptotic effect of ceramide is mediated by activation of different kinases and phosphatases, transcription factors and caspases. In many cases, it has been found that activation of components of family of MAPK (ERK, JNK and p38) (Verheij *et al.*, 1996) and inhibition of the phosphatidylinositol-3-kinase/Akt pathway (Salinas *et al.*, 2000) play important roles in apoptosis.

In summary, the roles of the different sphingolipids (ceramide, sphingosine, sphingosine-1-phosphate, etc.) in apoptotic pathways and the underlying mechanisms are obviously distinct: these sphingolipids act cooperatively in some cells, but in other cells they act oppositely or independently.

2.4. Mutants Strains Used in the Study

Mutants used in this study are *ino1Δ/ino1Δ*, *slc1Δ/slc1Δ* and *ser2Δ/ser2Δ* of wild type strain, BY4743, along with *INO1/ino1Δ*, *SLC1/slc1Δ*, *LCB2/lcb2Δ*, and *TSC2/tsc2Δ* mutants. These mutants are chosen with respect to the metabolic control analysis (MCA) performed on the yeast sphingolipid pathway (Kavun and Ülgen, 2005). According to that analysis, the enzymes encoded by the above mentioned genes were found to be the most critical ones affecting the ceramide concentrations in the pathway, and therefore chosen to be potential drug targets for cancer therapy.

2.4.1. *INO1* Gene and Its Function

The *INO1* gene encodes inositol 1-phosphate synthase, the enzyme that catalyzes the conversion of glucose 6-phosphate to inositol 1-phosphate.

$$\text{glucose 6-phosphate} \xrightarrow{\text{Ino1p}} \text{inositol 1-phosphate} \qquad (3.1)$$

During the logarithmic phase of growth, in the absence of inositol from the growth medium, this reaction is rate limiting for the synthesis of inositol-containing phospholipids (Griac and Henry, 1999). Inositol phosphates have been shown to play central roles in signal transduction pathways for a variety of neurotransmitters, hormones and growth factors and in mRNA export from nucleus (Dean-Johnson and Henry, 1989).

Expression of the *INO1* gene requires binding of Ino2p and Ino4p transcriptional activators to a repeated element, UASINO (Upstream Activating Sequence of INO) (Lopes *et al.*, 1991). This element is found in the promoters of *INO1* and other co-regulated genes (such as *CHO1*, *CHO2*) of the phospholipid biosynthesis pathway that are subject to regulation by inositol (Greenberg and Lopes, 1996). *INO1* transcription is a sensitive indicator of defects in the cellular transcription apparatus. Mutations in the large subunit of RNA polymerase II, the TATA binding protein (TBP), or components of the SWI/SNF chromatin remodeling complex lead to inositol auxotrophy (Ino-phenotype) due to an inability to activate the *INO1* gene (Shirra and Arndt, 1999). It is not yet known which proteins transmit the inositol signal to these transcriptional regulatory factors, due in part to the complexity of overlapping pathways that impinge on *INO1* expression.

2.4.2. *SLC1* Gene and Its Function

Slc1p is 1-acyl-sn-gylcerol-3-phosphate acyltransferase, it catalyzes the acylation of lysophosphatidic acid to form phosphatidic acid (Athenstaedt and Daum, 1999).

$$\text{PalCoA + G3P} \xrightarrow{\text{Slc1p}} \text{CoA + PA} \qquad (3.2)$$

SLC1 mutant suppresses sphingolipid long chain biosynthetic defect; the mutant also makes novel phosphatidylinositol derivatives and lacks sphingolipids.

The only acyltransferase involved in PtdOH formation of yeast that has been characterized at the molecular level so far is Slc1p. This protein was identified as an 1-

acyl-Gro3P AT by its ability to complement the PLSC deficiency in an *E. coli* mutant and by homology to this gene (Nagiec *et al.*, 1993).

Slc1p has a molecular mass of approximately 34 kDa and is thus of a size similar to 1-acyl-Gro3*P* ATs of *E. coli* (25 kDa). Localization studies with an *slc1*Δ strain demonstrated the presence of this enzyme in lipid particles, but similar to the putative Gat1p a portion of Slc1p was also detected in the ER (Athenstaedt and Daum, 1997). Slc1p is the only enzyme catalyzing conversion of lyso-PtdOH to PtdOH in the lipid particle fraction, but residual 1-acyl-Gro3P AT activity was detected in the microsomal fraction of the *slc1* deletion strain indicating the presence of additional 1-acyl-Gro3P ATs in this compartment.

2.4.3. *SER2* Gene and Its Function

Phosphoserine phosphatase of the phosphoglycerate pathway, Ser2p is involved in serine and glycine biosynthesis. Its expression is regulated by the available nitrogen source.

$$3PS + H_2O \xrightarrow{\text{Ser2p}} P + SER \qquad (3.3)$$

Amino acid biosynthesis may proceed via different metabolic routes in *Saccharomyces cerevisiae*. A possible route is to start biosynthesis of serine and glycine from the glycolytic intermediate 3-phosphoglycerate. The first reaction in this pathway, the "phosphoglycerate pathway," is catalyzed by phosphoglycerate dehydrogenase (EC 1.1.1.95), producing 3-phosphohydroxypyruvate plus NADH from 3-phosphoglycerate and NAD^+. The enzymes of the subsequent two reactions are phosphoserine transaminase (Ser1p, EC 2.6.1.52) and phosphoserine phosphatase (Ser2p, EC 3.1.3.3). Deletion mutants of either *SER1* or *SER2* need an external source of serine during growth on glucose (Belhumeur *et al.*, 1994). However, genes encoding the first enzyme of the pathway, phosphoglycerate dehydrogenase, have as yet not been identified in *S. cerevisiae* (Albers *et al.*, 2003).

2.4.4. *LCB2* and *TSC2 (LCB1)* Genes and Their Function

Tsc2p (Lcb1p) is component of serine palmitoyltransferase enzyme, responsible along with Lcb2p for the first committed step in sphingolipid synthesis, which is the condensation of serine with palmitoyl-CoA to form 3-ketosphinganine.

$$\text{PalCoA} + \text{H} + \text{SER} \xrightarrow{\text{Lcb2p, Tsc2p}} \text{KDHS} + \text{CoA} + \text{CO}_2 \qquad (3.4)$$

The first and committed step in *de novo* sphingolipid synthesis is catalyzed by serine palmitoyltransferase (SPT). Further reactions convert 3-ketosphinganine to the long-chain base sphingosine in animals and phytosphingosine in fungi and plants. *De novo* synthesis of sphingolipids in animals has been hypothesized to be controlled at the SPT step (Nagiec *et al.*, 1994). Experiments showing that treatment of neurons with a long-chain base decreases SPT activity support this hypothesis (Mandon *et al.*, 1991).

3. MATERIALS AND METHODS

3.1. Materials

3.1.1. Deletion Mutant Strains Adopted

The deletion mutant strains which were generated by EUROSCARF, were kindly provided by Prof. Stephen G. Oliver, Manchester.

A parent strain of *Saccharomyces cerevisiae*, BY4743, along with seven deletion mutant strains were grown and used as microorganisms: three homozygous deletion mutants of *ino1Δ/ino1Δ*, *slc1Δ/slc1Δ*, *ser2Δ/ser2Δ* and four heterozygous deletion mutants of *INO1/ino1Δ*, *SLC1/slc1Δ*, *LCB2/lcb2Δ* and *TSC2/tsc2Δ* were used in the experiments.

3.1.2. Maintenance of the Strains

Frozen stocks which were kept at -80^{o}C were prepared as follows: approximately fifty ml of complex (YPD) medium was inoculated with a single colony of cells grown on plates, and was incubated overnight at 30^{o}C and 180 rpm agitation. Then one ml of this preculture was saved in an eppendorf tube, mixed with one ml of 30 per cent (v / v) glycerol.

YPD agar plates, prepared as described in section 3.1.3, were inoculated with approximately 20 µl of preculture, prepared by growing frozen stocks previously mentioned in 50 ml YPD. The cells were spread evenly onto the plates using sterile spreading bar and they were left to grow at 30^{o}C overnight. The plates were then placed in the refrigerator, to 4^{o}C. To the YPD agar plates used for deletion mutants, 200 µg/ml of geneticin was added to enable the growth of geneticin resistant deletion mutants only.

YPD stock plates were prepared monthly to ensure their viability while frozen stocks were prepared and renewed twice a year.

3.1.3. Chemicals and Disposable Materials Used

3.1.3.1. Culture Media Yeast extract-peptone-dextrose medium (YPD) in solid (with agar) and liquid forms and F1 (limited) medium were used as culture media in the experiments. The compositions were weight per volume for solids and volume per volume for liquids:

- Composition of YPD Media (Solid and Liquid)

Yeast Extract 1 per cent (Lab M), Bacteriological Peptone 2 per cent (Acumedia), D-Glucose 2 per cent (Merck) – for solid media Agar-Agar 1.8 per cent (Merck). 40 per cent glucose was added from previously prepared stocks after sterilization of the remaining of the media.

- Composition of F1 Medium

D-Glucose 2.1 per cent (Merck), $(NH_4)_2SO_4$ 0.313 per cent (Merck), KH_2PO_4 0.2 per cent (Merck), $MgSO_4.7H_2O$ 0.055 per cent (Merck), NaCl 0.01 per cent (Merck), $CaCl_2.2H_2O$ 0.009 per cent (Merck), Uracil 0.002 per cent (Fluka), Histidine 0.002 per cent (Lifco), Leucine 0.01 per cent (Merck), Trace Element Solution 1 0.01 per cent, Trace Element Solution 2 0.01 per cent, Vitamin Stock Solution 0.17 per cent.

- Composition of Trace Element Solution 1

$ZnSO_4.7H_2O$ 0.07 per cent (Merck), $CuSO_4.5H_2O$ 0.01 per cent (Merck), H_3BO_3 0.01 per cent (Merck), KI 0.01 per cent (Merck)

- Composition of Trace Element Solution 2

$FeCl_3.6H_2O$ 0.05 per cent (BDH)

Vitamin stock solution was not steam sterilized, but filter sterilized. It was added by syringes on tip of which 0.22 μm filters were attached for sterilizing purposes to the of the rest of the medium without glucose. Previously steam sterilized glucose stock solution was added half an hour before inoculation to the medium to prevent undesired phenomena such as Malliard reactions or contamination.

- Composition of Vitamin Stock Solution

Inositol 3.72 per cent (Merck), Thiamine / HCl 0.84 per cent (Sigma), Pyridoxine 0.24 per cent (Fluka), Ca-panthothenate 2.4 per cent (Fluka), Biotin 0.018 per cent (Merck).

For *INO1* mutants grown in F1 medium, the vitamin stock mentioned above was prepared excluding inositol in order to prevent the inositol transport from the medium.

3.1.3.2. Glassware Required for the Analyses Since lipids are subject to corruption when contacting surfaces other than glass, metal or teflon, for pipetting purposes glass pipettes were used. Pasteur pipettes, micropipettes of volumes of 1-5, 10 and 20 µl were purchased from Hirschmann Laborgerate. Pyrex centrifuge tubes of 100 ml were purchased from DuPont.

3.1.3.3. Buffers and Chemicals Required for HPLC and TLC Applications All sphingolipid standarts were purchased from Sigma and Avanti Polar Lipids, HPLC grade chloroform, methanol, ethanol and n-hexane were obtained from Sigma. TLC plates used were 20 x 20 cm aluminium sheets coated with silica, fluorescent at 254 nm and were purchased from Merck.

Mobile phase which was required for HPLC analysis was as follows: HPLC grade Chloroform ($CHCl_3$)/Ethanol (EtOH)/Triethylamine (TEA)/Formic Acid(FA) (90:10:1:1 v/v). The concentrations for TEA and FA were 70 and 220 mM, respectively.

Mobile phase which was required for TLC analysis was as follows: HPLC grade Chloroform ($CHCl_3$)/Methanol (MetOH)/Acetic Acid (AA)/Water (H_2O) (25:15:4:2 v/v) for ceramide analysis and Chloroform ($CHCl_3$)/Methanol (MetOH)/Ammonium Hydroxide (NH_4OH) (40:10:1 v/v) for sphingoid base analysis. The concentration for NH_4OH was 2M.

3.1.4. Laboratory Equipment

- Autoclave ALP Model CL-40M (Japan)

- Balance — Precisa 80A-200M (Switzerland)
- Centrifuge — Avanti J-26 XPI Refrigerated Superspeed Centrifuge, Beckmann Coulter (USA)
- Deep freezers — -80^{o}C, New Brunswick Scientific U410 (England)
  -20^{o}C, BOSCH (Germany)
- HPLC System — 1515 Binary HPLC Pump, Waters (USA)
  717 plus Autosampler, Waters (USA)
  2420 ELSD, Waters (USA)
- Incubators — NÜVE EN500 (Turkey)
- Orbital Shakers — GFL 3032, GFL (Germany)
  INNOVA 4340 Illuminated refrigerated Incubator Shaker, New Brunswick Scientific (USA)
  EXCELLA E1 Open air shaker, New Brunswick Scientific (USA)
- Ovens — Incucell, MMM Group (Germany)
  VO 400 vacuum oven, Memmert (Germany)
- Refrigerators — +4^{o}C Arçelik (Turkey)
- Spectrophotometer — DU 640 Beckman (USA)
- Transilluminators — Foto/uv 15, Fotodyne (USA)
- Water Purification Systems — Millipore, Milli Ro Plus (USA)
  Millipore, Milli-Q UF Plus (USA)

3.2. Methods

3.2.1. Experimental Methods

3.2.1.1. Sterilization Contamination in any form, such as invasion of other organisms in the bioreactor, was prevented by sterilization during the experiments. Steam sterilization was performed in an autoclave at 15 psig pressure and 121^{o}C. Sterilized instruments were ensured to be kept sterile by taking appropriate measures into account, such as sealing the necks of bottles, use of sterile gloves while working, use of a sterile fume hood in which Bunsen burners were lit for inoculation processes.

The culture medium as well as stock solutions of mediums was steam sterilized for 15 min. at previously described settings. Glucose stock solution however, was sterilized only 3 min, because of the risk of caramelization. All plastic tips and tubes, glass pipetting material, erlenmeyers etc. that were to be used were steam sterilized for 20 minutes at 15 psig and 121 °C. Filter sterilization was also adopted for adding vitamin from its stock solution to F1 medium, using 0.22 µl Millipore filters.

3.2.1.2. Cultivation Conditions All precultures were prepared as 50 ml of YPD medium corresponding to 10 per cent of the volume of the batch culture. They were harvested with a single colony of cells from YPD agar plates. The colonies were inoculated via single use, disposable plastic inoculation sticks. The precultures were incubated in orbital shakers at 30^{o}C and 180 rpm. The preculture was ready to be used at its late exponential phase when the optical density was measured to be between 0.9 and 1.1.

Batch cultivations were carried out in 500 ml Erlenmayer flasks with a cultivation volume of 120 ml of YPD medium. The experiments were carried out at 30^{o}C and 180 rpm in orbital shakers. 1-2 ml of preculture was used to inoculate the culture. The pH was kept between 5.5 and 6.5. Samples were collected on an hourly basis and checked whether steady state is reached, then steady state samples were collected at about 24th h of the experiment.

3.2.1.3. Determination of the Cell Dry Weight The optical density was determined by the UV spectrophotometer at a wave length of 600 nm.

Petri dishes with filter papers in them were numbered and left in the oven at 70°C overnight. The dishes were then cooled and placed in the desiccator and left there for 1-2 hours prior to use. After the weight measurement of these completely dried dishes, a known volume of sample was pipetted in them and these cell containing dishes were dried at 70°C for a day. These dishes were again cooled and left in the dessicator before the second weight measurement. The difference between the two measurements gives the cell dry weight. In order to be more accurate, three measurements are done for each culture, and the average of these values are taken as dry cell weight.

3.2.1.4. Lipid Extraction Two different lipid extraction procedures were carried out since it was not clear which one of them would give the best results. In order to be able to choose between them, a verification step was performed by using TLC.

For the first extraction procedure which was kindly provided by Jens Nielsen's laboratory, the cells were first harvested by centrifuging for 5 min at 3000 rpm and 4°C and the supernatants was discarded. The pellet was resuspended in deionized water and the centrifugation was repeated and the sample was left to freeze at -20°C overnight. Then 12 ml of $CHCl_3$: MeOH (1:2) was added to the frozen pellets and the samples were shaken for 3 hr at 4ºC with Excella E1, benchtop open air shaker, at medium speed. After three hours, 4 ml $CHCl_3$ and 4 ml 0.73 per cent (w/v) NaCl was added. Samples were shaken again for about 15 min., at submedium speed. It was observed that two phases were formed and lower phase was taken with the aid of a Pasteur pipette and it was saved in another glass tube. To the remaining cell extracts, 6 ml of $CHCl_3$:MeOH 85:15 (v/v) was added, samples were left overnight at 4ºC and the next day lower phase was collected. This step was repeated two times. Finally, solvent of the extracted lipids was evaporated at 40ºC under vacuum (~ 300 mb). Dried lipids were resuspended in 500 µl of $CHCl_3$: MeOH 2:1 (v/v). All centrifugations were performed using Avanti J-26 XPI, Beckman-Coulter centrifuge with JA-14 rotor.

For the second extraction procedure which was a modified version of Bligh and Dyer process (Bligh and Dyer, 1959), the cells were first harvested by centrifuging for 5 min at 2000 rpm at room temperature and the supernatants were discarded. The sample was left to freeze at -20°C overnight. 3 ml glass beads and 15 ml $CHCl_3$: MeOH 2:1 (v/v) was added to the frozen pellets and samples were shaken on platform mixer at maximum speed for 10 min at 4ºC. Then 3 ml 0.034 per cent MgSO4 (w/v) was added and extracts were shaken at sub-max speed for 30 min at 4ºC. Samples were centrifuged at 2000 rpm for 5 min at room temperature. Upper phase was discarded. 6 ml of H_2O:MeOH:$CHCl_3$ 47:48:3 (v/v) was added to each sample. Centrifugation and upper phase elimination were repeated. Organic phase of the samples (lower phase but not the glass beads) was transferred to glass tubes. Glass beads were washed with 6 ml MeOH: $CHCl_3$ 1:2 (v/v) and vortexed for 5 min. Samples were centrifuged at 2000 rpm for 5 min at room temperature. Organic Phase was transferred to tubes. Samples were kept overnight at 40ºC under vacuum to evaporate the solvent. Dried samples (lipids) were dissolved in 500 µl of $CHCl_3$:MeOH 2:1 (v/v). All centrifugations were performed using Avanti J-26 XPI, Beckman-Coulter centrifuge with JA-14 rotor.

3.2.1.5. Extraction Method Determination by TLC The stationary phase in TLC was silica plates on aluminium with fluorescent marker (Fluka) while mobile phase was Chloroform/Methanol/Acetic acid/Water 25:15:4:2 (v/v). Two different TLC methods differing in the activation of TLC plates were used.

- Acetone-activated Plates: TLC plates were left in acetone bath for 1 hr for activation.
- Heat-activated Plates: TLC plates were heated in the oven at 115ºC for 15 min.

After TLC plates were activated, cell extracts were spotted to the bottom of the plates using 10 µl pipettes. These plates were then left in TLC tank with mobile phase until the solvent diffused to top of the plates. Processed plates were dried and lipids were detected with Foto/UV 15 transilluminator.

3.2.1.6. HPLC Analysis of the Extracted Lipids HPLC analysis of lipids were performed using a 3 µm C_{18} Silica column (4.6x150 mm) and a guard column of the same material

(4.6x25 mm) provided by Waters. The components of the HPLC system were described in the equipment list and the parameters used with the system are given in Table 3.1 (McNabb *et al.*, 1999). ELSD detector was used with nitrogen gas at high pressure. Isocratic elution procedure was adopted in HPLC analysis.

Table 3.1. Parameters of the HPLC system

Flowrate (ml/min)	0.5
Column Temperature (^{0}C)	25
Gain	6
Gas Pressure (bar)	1.9
Drift Tube Temperature (^{0}C)	70

Various injection volumes were tried for sample analysis, and the optimum value for yeast lipid extracts was found to be 40 µl. For lipid standards purchased from Sigma and Avanti, multiple injections with different injection volumes were carried out in order to construct a calibration curve for each standard which enabled the direct connection between their concentration and peak area on the chromatogram.

Prior to injection, column and guard column were washed with 20 column volumes of HPLC grade methanol, ~ 25 ml, and every week they were cleaned with again 20 column volumes of HPLC grade n-hexane. While the column was being washed with methanol, the mobile phase, the composition of which was given in section 3.1.3.3, was prepared and degassed under helium sparging for about 20 min. The standards dissolved in HPLC grade chloroform and the extracted lipids to be analyzed were diluted so that the final analytes were chloroform/ethanol 9:1 (v/v).

The chromatography adopted in the study was a normal phase HPLC which was separating analytes based on polarity. The polar stationary phase was silica and the nonpolar mobile phase was $CHCl_3$/EtOH mixture namely. The polar analyte, lipids, associated with and was retained by the polar stationary phase. Adsorption strengths increased with analyte polarity, and the interaction between the polar analyte and the polar stationary phase (relative to the mobile phase) increased the elution time. This effect was observed and considered while discussing the chromatograms of extracted lipids.

4. RESULTS AND DISCUSSION

In order to investigate the mechanisms involved in sphingolipid synthesis, deletion mutants of the genes involved in sphingolipid pathway were studied by batch experiments. Current study is the experimental part of an existing project which also has a computational part that investigates sphingolipid mechanism. The results stated here aim to gain further insight on sphingolipid synthesis mechanism and to qualify as well as to quantify sphingolipid species in *S. cerevisiae* with an ultimate goal of determination of potential drug targets developped by computational methods. BY4743 wild type strain and four different heterozygous strains as well as three different homozygous strains, *INO1/ino1Δ*, *SLC1/slc1Δ*, *LCB2/lcb2Δ*, *TSC2/tsc2Δ* (*LCB1/lcb1Δ*), *ino1Δ/ino1Δ*, *slc1Δ/slc1Δ* and *ser2Δ/ser2Δ* were used in order to explore the effect of gene deletions on sphingolipid production by *S. cerevisiae*.

Wild type strain as well as the seven mutant strains were grown in YPD. To be able to distinguish the effect of nutrient uptake -from medium into the cell- of vital compounds such as serine and myo-inositol (which were readily present in complex medium) for sphingolipid synthesis minimal media were also used. Wild type strain and three homozygous strains, *ino1Δ/ino1Δ*, *slc1Δ/slc1Δ* and *ser2Δ/ser2Δ* were grown in F1 medium lacking serine but containing inositol at a known concentration, 0.556 mg/L. For *ino1Δ/ino1Δ* only, F1 medium without inositol was also adopted as culture medium.

Experiments were carried out batchwise in 500 ml erlenmeyer flasks with a working volume of 110 ml at 30 ºC and 180 rpm. 100 ml samples were taken for lipid extraction and 1 ml samples were collected for dry weight measurements when cells reached stationary phase.

To choose the most appropriate lipid extraction method out of the two methods stated in section 3.2.1.4, a TLC analysis was performed. This analysis also included determination of the best TLC method for sphingolipid analysis, both for ceramides and sphingoid bases.

For the quantification and qualification of yeast sphingolipids, standards of PHS, C18-DHS, C20-DHS, P-Cer, C2-Cer, C6-Cer and C8-Cer were used. Purchased sphingolipid standards were loaded to HPLC to get their specific retention time for qualification process and peak chromatograms in response to injection concentration. The area under each chromatogram was calculated to obtain the calibration curves for each standard to be used in the quantification of yeast extracted sphingolipids.

It was not possible to have all the standards of yeast extracted sphingolipids as the commercially available standards were primarily mammalian sphingolipids. However, analogies were made between some of the standards and yeast sphingolipids based on the molecular weights and the polarity, since they were the main parameters of HPLC instrumentation used for separation and detection of the lipids. Furthermore, by comparing chromatograms of various strains, retention time values for complex ceramides in yeast such as inositol-phosphoryl-ceramide -IPC-, mannosyl-inositol-phosphoryl-ceramide –MIPC-, and mannosyl-diinositol-phosphoryl-ceramide -$M(IP)_2C$- were annotated.

4.1. Growth Characteristics of the Wild Type and Mutant Strains of *S. cerevisiae*

Biomass (g/l) values of wild type strain and seven mutant strains grown in different media were given in Table 4.1. The biomass values were calculated according to the procedure given in section 3.2.1.3. Stationary phase samples were collected and used for biomass determination.

From Table 4.1, it was observed that in YPD medium, wild type strain had overgrown all the mutant strains except *slc1Δ/slc1Δ* mutant. The lowest biomass value, 4.42 g/l, belonged to *ser2Δ/ser2Δ* mutant. Homozygous *ino1Δ/ino1Δ* mutant had also a relatively low biomass value with respect to the four remaining heterozygous mutants grown in YPD medium, *INO1/ino1Δ*, *SLC1/slc1Δ*, *LCB1/lcb1Δ* and *LCB2/lcb2Δ* which possessed biomass values close to 4.60-4.70 g/l.

For F1 medium, both *ino1Δ/ino1Δ* and *slc1Δ/slc1Δ* mutants had overgrown wild type strain interestingly. Only *ino1Δ/ino1Δ* mutant grown in F1 medium without inositol had the lowest biomass value (1.78 g/l) among all the biomass values of all strains.

Table 4.1. Biomass (g/l) values of strains grown in different media

	YPD	**F1**	**F1 without inositol**
Wild Type	5.45	4.27	-
ino1Δ/ino1Δ	4.54	4.28	1.78
INO1/ino1Δ	4.63	-	-
slc1Δ/slc1Δ	5.77	4.62	-
SLC1/slc1Δ	4.73	-	-
ser2Δ/ser2Δ	4.42	-	-
LCB1/lcb1Δ	4.73	-	-
LCB2/lcb2Δ	4.65	-	-

4.2. Optimization of Lipid Extraction Procedure by TLC

As stated in section 3.2.1.5, two different TLC methods differing in the activation of TLC plates were used in order to optimize the lipid extraction processes: acetone activation and heat activation. The activation method which gave the best lipid bands visualised by UV transilluminator was adopted in the ongoing work.

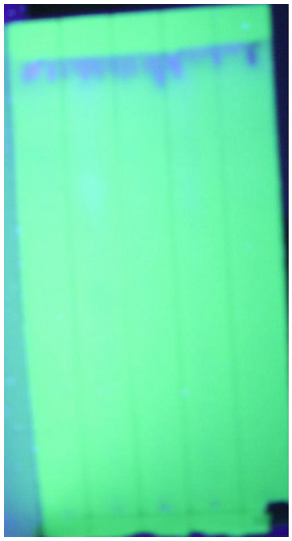

Figure 4.1. Acetone activated TLC results with procedure #1 extraction

Figure 4.2. Acetone activated TLC results with procedure #2 extraction

Any bands could not be detected on Figure 4.1 and Figure 4.2. Hence, it was concluded that acetone activated plates were not suitable for TLC analysis in this work.

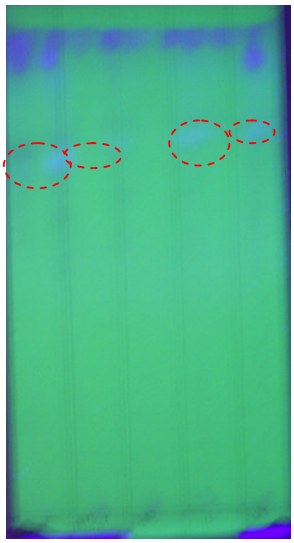

Figure 4.3. Heat activated TLC results with procedure #1 extraction

It was observed from Figure 4.3 and Figure 4.4 that some bands could be seen on the TLC plates with the first extraction procedure. It was concluded that lipid extraction with the first procedure when compared to the second procedure gave better results on *S. cerevisiae* cells as well as heat-activated plates must be used instead of acetone-activated ones.

Figure 4.4. Heat activated TLC results with procedure #2 extraction

4.3. Detection of Sphingolipid Standards by HPLC

In order to be able to qualify and quantify yeast sphingolipids, standards purchased from Sigma and Avanti were injected to HPLC system at different concentrations. Hence, the retention time for each specific standard as well as the effect of its concentration on the peak area of the chromatogram obtained by HPLC was determined. Then, a calibration curve for each standard, which would be referred to later in the quantification and qualification of yeast sphingolipids, was constructed by fitting a trend line on the graph of concentration vs. peak area.

The standards used in the work were PHS, C_{18} DHS, C_{20} DHS, C_2 Ceramide, C_6 Ceramide, C_8 Ceramide and C_2 Phytoceramide. These standards, except from PHS and C_2 Phytoceramide which were the only commercially available sphingolipids obtained from yeast, were purified from mammalian cells. However, they were analogous to yeast sphingolipids.

The molecular properties and functions of these commercial standards analyzed are given in Table 4.2.

Table 4.2. Functions and properties of sphingolipid standards

Abbreviation	Name	Function	Molecular Formula	Molecular Weight	Structure
C2-Cer	Acetyl ceramide	Cell-permeable, biologically active ceramide. Induces differentiation and apoptosis and activates protein phosphatases	$C_{20}H_{39}NO_3$	341.53	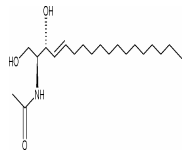
C6-Cer	Caproyl ceramide	Cell-permeable analog of ceramide; activates MAP kinase; induces apoptosis in human leukemia HL-60 cells	$C_{24}H_{47}NO_3$	397.63	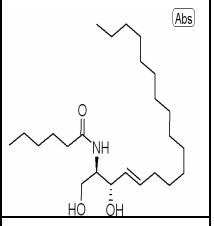
C8-Cer	N-Octanoyl-D-sphingosine	Synthetic analogue of natural ceramide, activates protein kinase C, stimulates IL-2 production and induces apoptosis.	$C_{26}H_{51}NO_3$	425.69	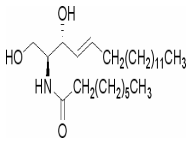
C-20 DHS	D-*erythro*-Sphinganine (C20)	Biosynthetic precursor to sphingosine; inhibits protein kinase C	$C_{20}H_{43}NO_2$	329.561	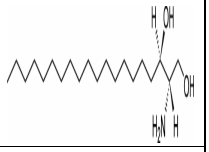
C-18 DHS	N-Stearoyl-D-*erythro*-Sphinganine	Most common sphingoid base in mammalian tissues, precursor to DHCer, GPI anchoring ceramide.	$C_{36}H_{73}NO_3$	567.97	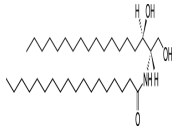
P-cer	Phyto ceramide C2	Yeast growth inhibitor and ceramide-activated protein phosphatase (CAPP) activator	$C_{20}H_{44}NO_4$	359.54	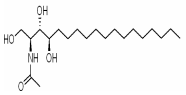
PHS	N-Stearoyl-Phyto sphingosine	Involved in mediating the heat stress response. It is proapoptotic in human cancer cell lines.	$C_{36}H_{73}NO_4$	583.554	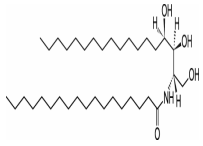

4.3.1. C8-Cer

C8-Cer, namely D-*erythro*-N-Octanoyldihydrosphingosine was one in the series of short acyl chain lengths synthetic analogs of natural C16 ceramide. Synthetic, cell permeable ceramides and ceramidephosphates analogs were used to study intracellular signaling, cell migration, cell death, and modulation of protein kinase C activity (PKC). Synthetic ceramides exist in four stereoisomers: *D-erythro, D-threo, L-erythro and L-threo*, of which only *d-erythro*–ceramide occurs in nature. D-*erythro*-isoform is 10 times more active than L-*threo*-isoform. C8-Cer purchased from Sigma was injected to HPLC to have its chromatogram.

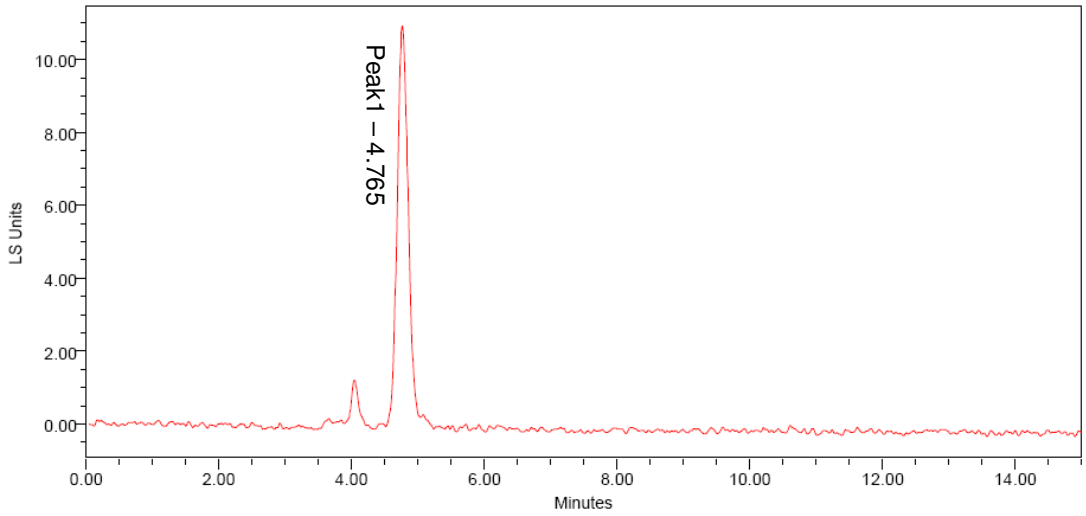

Figure 4.5. Autoscaled chromatogram of C8-Cer

As can be seen on Figure 4.5, the residence time for C8-Cer was about 4.7 min. However, during the multiple injections, it was seen that it differed from 4 min to 4.8 min. This shift in the retention time was probably due to the particle loading in the column and instantaneous flowrate changes in the mobile phase. This figure was the chromatogram of 0.05 mg/ml (0.00012 mM) C8-Cer. Aside from this injection, an injection of 0.0005 mg/ml and two injections of 0,000005 mg/ml were also carried out and their response chromatograms were obtained. The results given in Table 4.3 were used in the construction of calibration curve (Figure A.1).

Table 4.3. Injection results of C8-Cer

Area (µV*sec)	**Height (µV)**	**Amount (mg)**
4954	674	5×10^{-6}
6436	1046	5×10^{-4}
15980	601	5×10^{-3}
131310	11023	5×10^{-2}

4.3.2. C6-Cer

C6-Cer, namely caproyl ceramide purchased from Sigma was injected to HPLC to have its chromatogram.

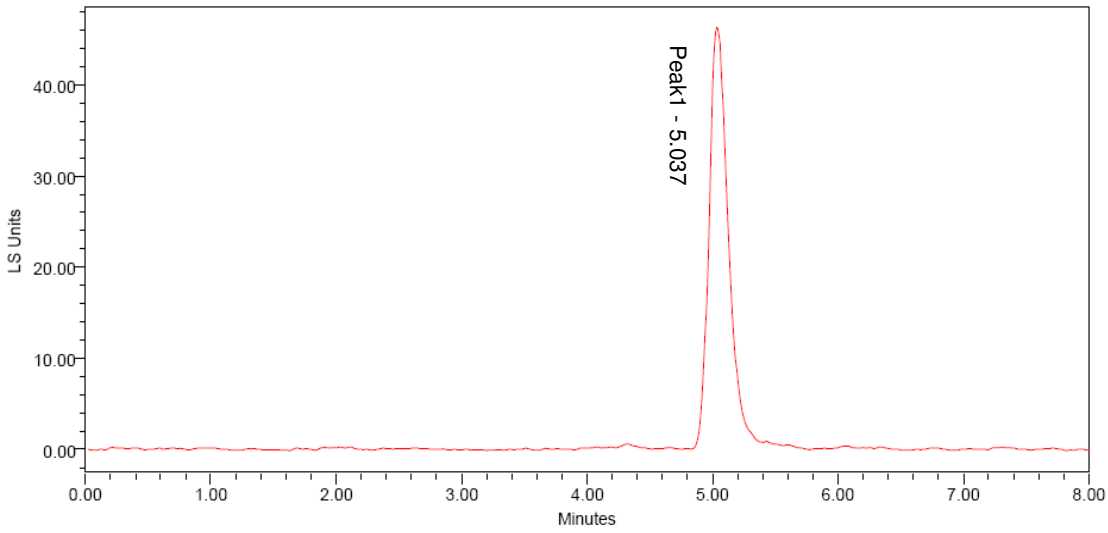

Figure 4.6. Autoscaled chromatogram of C6-Cer

From Figure 4.6, the residence time for C6-Cer was observed to be about 5 min. This figure was the chromatogram of 0.1 mg/ml (0.000251 mM) C6-Cer. Aside from this injection, two injections of 0.0005 mg/ml, one injection of 0.05 mg/ml, one injection of 0.0002 mg/ml and one injection of 0.00004 mg/ml were also accomplished and their response chromatograms were obtained. The results are given in Table 4.4. Calibration curve plotted is on Figure A.2.

Table 4.4. Injection results of C6-Cer

Area (µV*sec)	Height (µV)	Amount (mg)
60808	3085	4×10^{-8}
18352	2159	5×10^{-7}
25082	2441	5×10^{-7}
15754	1552	2×10^{-7}
266688	33268	5×10^{-5}
488630	46133	1×10^{-4}

4.3.3. C2-Cer

C2-Cer, namely acetyl ceramide was a less hydrophobic analog of natural ceramides, which made it an active cell permeable surrogate. This semisynthetic ceramide analog purchased from Sigma was injected to HPLC to have its chromatogram.

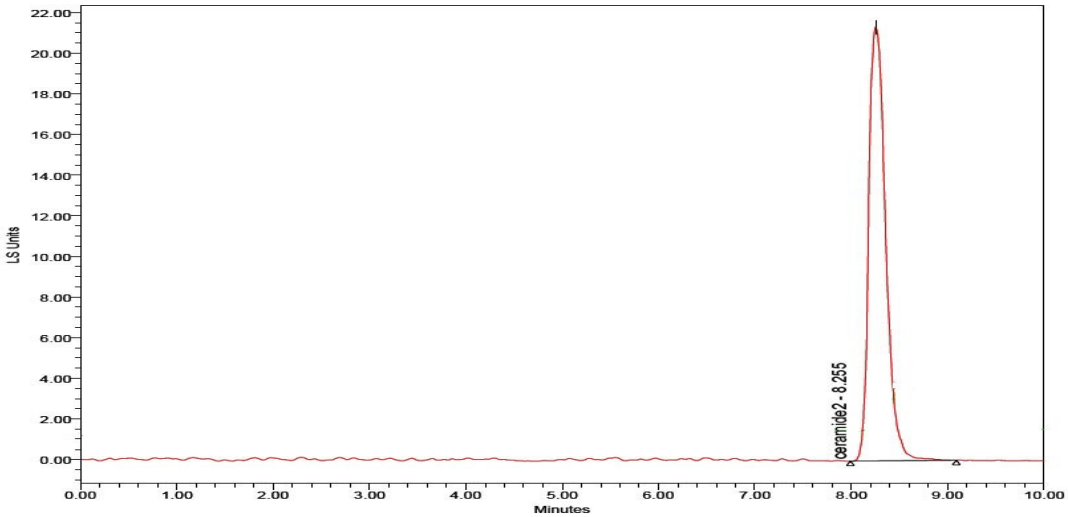

Figure 4.7. Autoscaled chromatogram of C2-Cer

The residence time for C2-Cer is about 8.2 min, shown on Figure 4.9. However, during the multiple injections, it was seen that it differed from 7.9 min to 8.6 min. This shift in the retention time was probably due to the particle loading in the column and instantaneous flowrate changes in the mobile phase.

Figure 4.7 belongs to the chromatogram of 0.05 mg/ml (0.000146 mM) C2-Cer. Aside from this injection, an injection of 0.0005 mg/ml, an injection of 0.005 mg/ml and one injection of 0,000005 mg/ml were also performed and their response chromatograms were obtained. The results given in Table 4.5 were used in the construction of calibration curve shown in Figure A.3.

Table 4.5. Injection results of C2-Cer

Area (µV*sec)	**Height (µV)**	**Amount (mg)**
810	47	5×10^{-9}
5841	479	5×10^{-7}
796090	54138	5×10^{-6}
2392663	113553	5×10^{-5}

4.3.4. P-Cer

P-Cer, namely C_2 Phytoceramide purchased from Sigma was injected to HPLC to have its chromatogram at three different concentrations: 0.01 mg/ml, 0.02 mg/ml and 0.04 mg/ml. The results given in Table 4.6 were used in the construction of calibration curve (Figure A.4).

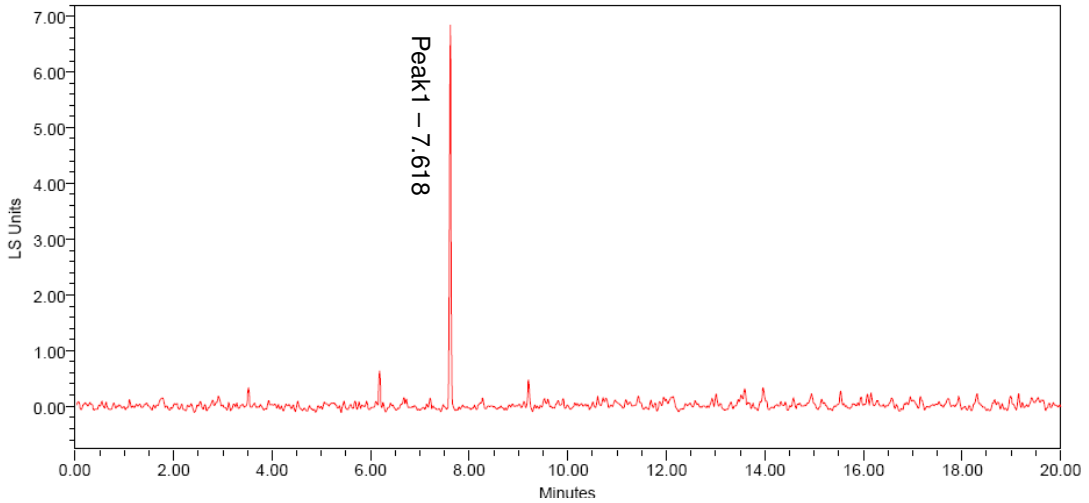

Figure 4.8. Autoscaled chromatogram of P-Cer

From the chromatogram given in Figure 4.8, it is seen that the retention time for C_2 phytoceramide is about 7.6 min. Yet, it was seen that the retention time differed from 7.6 min to 8 min during multiple injections. This shift in the retention time was probably due to the particle loading in the column. The chromatogram of 0.04 mg/ml (0.00011 mM) of C_2 phytoceramide is given in Figure 4.11.

Table 4.6. Injection results of P-Cer

Area (µV*sec)	**Height (µV)**	**Amount (mg)**
1615	183	1×10^{-5}
1819	232	2×10^{-5}
15297	6809	4×10^{-5}

4.3.5. PHS

PHS, namely N-Stearoyl-Phyto sphingosine, purchased from Avanti was injected to HPLC to have its chromatogram.

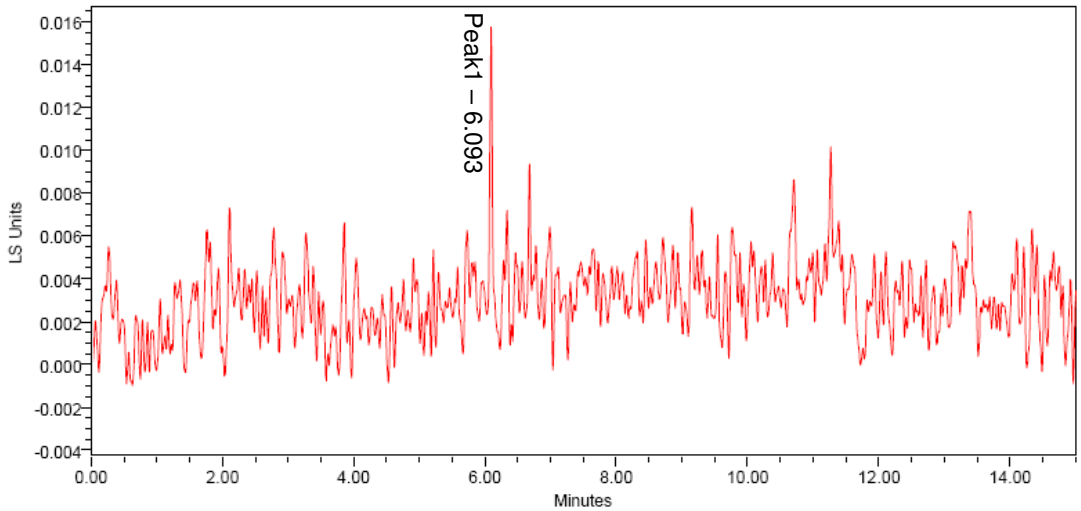

Figure 4.9. Autoscaled chromatogram of PHS

It is observed that the residence time for PHS is about 6 min (Figure 4.9). However, during the multiple injections, it was seen that it differed from 5.8 min to 6.8 min.

This shift in the retention time was probably due to the particle loading in the column. Figure 4.9 belongs to the chromatogram of 0.00005 mg/ml (8.6 10^{-8} mM) PHS. Aside from this injection, two other injections of 0.00005 mg/ml, two injections of 0,0005 mg/ml and one injection of 0.01 mg/ml were also tested and their response chromatograms were obtained. The results are given in Table 4.7. With these data points, the calibration graph constructed is given in Figure A.5.

Table 4.7. Injection results of PHS

Area (µV*sec)	**Height (µV)**	**Amount (mg)**
40	14	5 x 10^{-8}
76	15	5 x 10^{-8}
127	58	5 x 10^{-8}
235	16	5 x 10^{-6}
245	71	5 x 10^{-6}
638	130	1 x 10^{-5}

4.3.6. C18-DHS

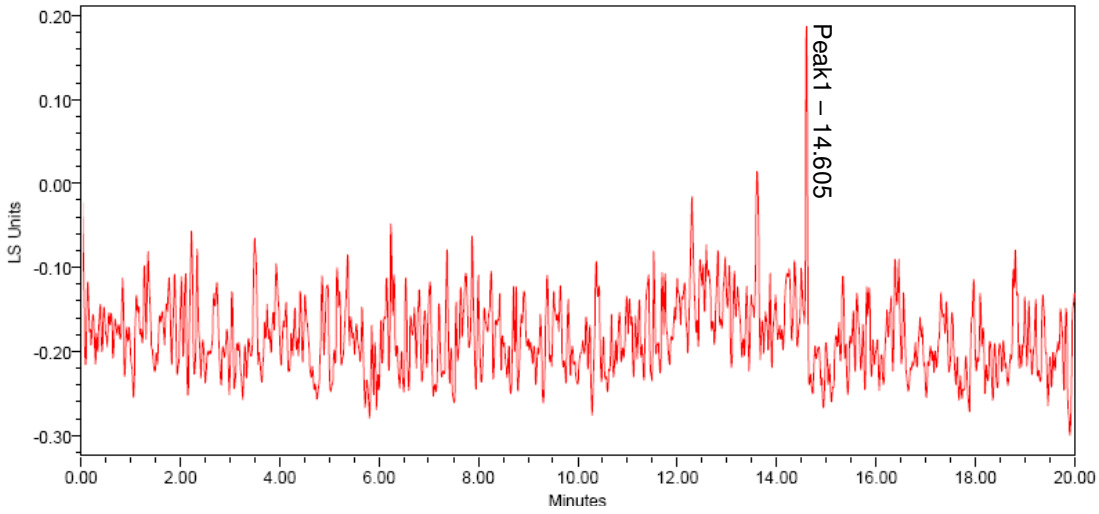

Figure 4.10. Autoscaled chromatogram of C18-DHS

C18-DHS, namely N-Stearoyl-D-*erythro*-Sphinganine, purchased from Avanti was injected to HPLC to have its chromatogram.

As it can be seen on Figure 4.10, the residence time for C18-DHS is about 14 min. However, during the multiple injections, it was seen that it differed from 14 min to 16 min. The above figure was the chromatogram of 0.01 mg/ml (1.8 10^{-5} mM) C18-DHS. Aside from this injection, an injection of 0,02 mg/ml and an injection of 0.005 mg/ml were also tested and their response chromatograms were obtained. The results, which were used in the construction of calibration curve given in Figure A.6, are given in Table 4.8.

Table 4.8. Injection results of C18-DHS

Area (µV*sec)	**Height (µV)**	**Amount (mg)**
129	22	5 x 10^{-6}
1707	350	1 x 10^{-5}
8893	3938	2 x 10^{-5}

4.3.7. C20-DHS

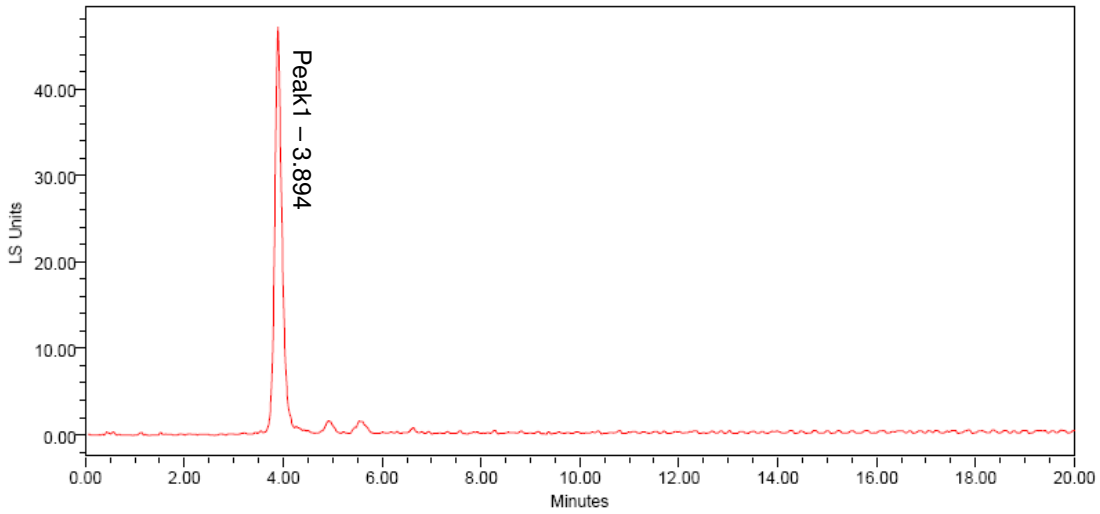

Figure 4.11. Autoscaled chromatogram of C20-DHS

C20-DHS, namely D-*erythro*-Sphinganine, purchased from Avanti was injected to HPLC to have its chromatogram. As it can be seen on Figure A.7, the residence time for C20-DHS is about 3.9 min.

However, during the multiple injections, it was seen that it differed from 3.9 min to 4.4 min. This shift in the retention time was probably due to the particle loading in the column and instantaneous flow rate changes in the mobile phase. This figure was the chromatogram of 0.05 mg/ml (0.000152 mM) C20-DHS. Aside from this injection, another injection of 0.05 mg/ml and two injections of 0,025 mg/ml were also tested and their response chromatograms were obtained. The results given in Table 4.9 were used in the construction of calibration curve (Figure A.7).

Table 4.9. Injection results of C20-DHS

Area (μV*sec)	**Height (μV)**	**Amount (mg)**
35831	3137	2.5×10^{-5}
30637	1851	2.5×10^{-5}
492038	47032	5.0×10^{-5}
529300	12678	5.0×10^{-5}

4.4. Qualificaiton and Quantification of Sphingolipids of *S. cerevisiae* Strains

Extracted lipid moiety from each strain was loaded to HPLC and their chromatograms were analyzed. For qualification process, retention time values were taken as a basis. Comparing the standards injected and yeast sphingolipid profiles, peaks on the yeast chromatograms were annotated to a standard by checking the retention time similarity. Also, the amount of these annotated lipids in the specific strain were predicted by observing their response areas on the chromatogram and the calibration equations previously constructed for the quantification process. Hence, the area values given on the response chromatogram were converted to concentration values for each species by using calibration curves.

4.4.1. Peak Annotation and Determination for Yeast Sphingolipids

Chromatograms of different deletion mutants were investigated to determine the sphingolipids in yeast corresponding to standards as well as to annotate peaks to IPC,

MIPC and $M(IP)_2C$. Among the standards used, it was known that C18-DHS, PHS and P-Cer were standing for DHS, PHS and phytoceramide, P-Cer in yeast respectively.

Table 4.10. Sphingolipid concentrations for BY4743 at steady-state (Alvarez-Vasquez *et al.*, 2005)

Metabolite	**Concentration (mol per cent)**
DHS	0.0100
D-Cer	0.0360
DHS-P	0.0010
PHS	0.0500
PHS-P	0.0050
P-Cer	0.0520
IPC	0.1020
MIPC	0.1400
$M(IP)_2C$	0.0085

Wild type sphingolipid concentrations in mole per cents, concentration of sphingoid base or phosphatidate over concentration of total phospholipid, were available in literature (Table 4.10) which enabled the determination and annotation process.

Sphingolipid chromatogram of wild type strain grown in YPD medium was given in Table 4.11. According to this chromatogram, some of the peaks which had retention time values matching with the standards tested were identified.

C8-Cer was attributed to IPC and C2-Cer was attributed to DHS-P in yeast because of the polarity similarities between these compounds. The HPLC system adopted was a normal phase HPLC, hence it detected and separated lipids according to polarity. When Figure 4.12 was observed, it was seen that although carbon chain lenghts differed between C8-Cer and IPC, the groups required for the polarity such as –OH groups and =O bond, were quite in accordance with each other.

Table 4.11. Peak results for BY4743 grown in YPD

Peaks	Retention Time (min)	Area (µVxsec)	Standard Matched	Possible Compound
1	5.361	2077	C8-Cer	IPC
2	7.029	4480	PHS	PHS
3	7.613	2991		
4	7.957	9467	P-Cer	P-Cer
5	10.146	8405	C2-Cer	DHS-P
6	11.283	5198		
7	13.433	21959		
8	16.515	4994		
9	18.235	6490		

In Figure 4.12 (a), there was a slight polarity at the left end of the molecule, due to the negatively charged oxygen element bonded to the phosphorus. The cylic part bounded was apolar since it was cyclic and the –OH groups were bounded to carbon atoms present at the edges. Hence the –OH groups were organized such that they neutralized each other at this location. Further more, there were two –OH groups bonded to the upper leg while just one –OH group was bonded to the other leg of the molecule.

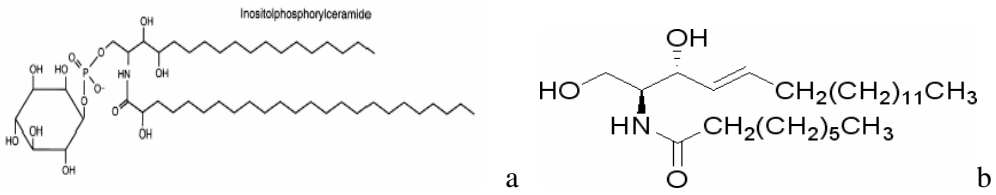

a b

Figure 4.12. Structures of ceramides (a) inositol-phosphorylceramide and (b) C8-Cer

When Figure 4.12 (b) was observed, it was seen that again a slight polar nature was present at the left end due to the presence of an –OH group, and one –OH group was bonded to the upper leg. So, in overall polarity these two molecules resembled each other, which rendered the detection of IPC by the presence of C8-Cer in yeast. This analogy aaumption was also tested by the absence of C8-Cer on the chromatogram of *ino1Δ/ino1Δ* grown in F1 without inositol medium.

When Figure 4.13 (a) and (b) were compared, it was noticed that the polarity due to =O group in both of the figures was similar. Besides from the polarity, the molecular weight of C2-Cer and DHS-P were also close to each other, which rendered the detection of DHS-P in yeast by the presence of C2-Cer peaks in its chromatogram.

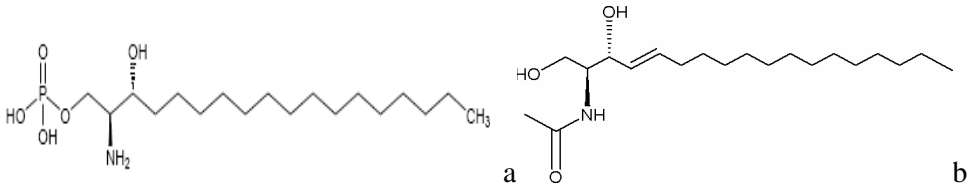

Figure 4.13. Structures of sphingolipids (a) DHS-P and (b) C2-Cer

When wild type strain grown in YPD and *ino1Δ/ino1Δ* mutant were grown in F1 without inositol media, their chromatograms differed especially in complex sphingolipids, IPC, MIPC and $M(IP)_2C$. Thus, the peak areas and retention times given in Table 4.11 and Table 4.12 were analyzed according to these differences.

Table 4.12. Peak results for *ino1Δ/ino1Δ* grown in F1

Peaks	**Retention Time (min)**	**Area (μVxsec)**	**Standard Matched**	**Possible Compound**
1	6.281	202	PHS	PHS
2	6.777	146	P-Cer	P-Cer
3	7.558	94		
4	10.148	56	C2-Cer	DHS-P
5	18.136	96		
6	18.989	156		

From the comparison of Table 4.11 and Table 4.12, it was seen that *ino1Δ/ino1Δ* chromatogram lacked two peaks with retention time values of 13.175 min and 16.772 min which were present in wild type chromatogram. Hence, these two retention times were proposed to be representing the peaks of MIPC and $M(IP)_2C$ respectively. Also, the retention time of 18.235 min on Table 4.11 was assumed to belong to D-Cer. The reason for this assumption is that its per cent concentration was close to that of P-Cer from Table 4.10 and so was its area value on Table 4.11.

With these annotations, wild type strain's (grown in YPD) sphingolipid chromatogram profile was investigated to check the reliability of these assumptions, since the sphingolipid proportions for this strain were available (Table 4.10). The per cent concentrations given in Table 4.10 were divided by that of PHS and thus converted to proportions of sphingolipids for wild type strain. The results of the qualification and the quantification of sphingolipids for wild type strain grown in YPD were given in Table 4.13. Using these experimental concentrations, proportions of individual sphingolipids to PHS were calculated and compared to the values given in the literature.

From Table 4.14, one could conclude that the experimental values were in good accordance with the ones given in literature. So, the amounts for MIPC, $M(IP)_2C$ and D-Cer in the other deletion mutant strains were calculated with respect to these values for wild type strain and replaced with the experimental values. Also, an assumption was made that the concentrations of these compounds changed linearly with the peak areas. Then, from the "calculated" experimental values of MIPC, $M(IP)_2C$ and D-Cer in wild type strain grown in YPD, concentrations in the other strains were calculated on the basis of this assumption.

Table 4.13. Sphingolipid profile of BY4743 grown in YPD

Peaks	**Retention Time (min)**	**Area (μVxsec)**	**Standard Matched**	**Experimental Concentration (mM)**	**Possible Compound**
1	5.361	2077	C8-Cer	0.048562076	IPC
2	7.029	4480	PHS	0.002978713	PHS
3	7.613	2991			
4	7.957	9467	P-Cer	0.003466788	P-Cer
5	10.146	8405	C2-Cer	4.90646E-05	DHS-P
6	11.283	5198			
7	13.433	21959			MIPC
8	16.515	4994			$M(IP)_2C$
9	18.235	6490			D-Cer

Table 4.14. Comparison of experimental data with literature for BY4743 grown in YPD

	Proportions in Literature for BY4743 in YPD	**Experimental Proportions For BY4743 in YPD**
D-Cer/PHS	0.798	
DHS-P/PHS	0.020	0.016
P-Cer/PHS	1.054	1.164
IPC/PHS	22.938	16.303
MIPC/PHS	2.799	
$M(IP)_2C$/PHS	0.170	

4.4.2. Sphingolipid Qualification and Quantification for BY4743

Wild type strain was grown in YPD and F1 separately to see the effect of uptake reactions. Since YPD medium was a rich medium in terms of amino acids such as serine, or other vital compounds, such as inositol, present in the yeast extract in unknown amounts, it was expected that sphingolipid amounts of wild type strain grown in YPD would be higher than the quantity of sphingolipids of wild type strain grown in F1 medium which was a limited medium compared to YPD. Indeed this was the case, which could be observed from Figure 4.14 and Figure 4.15.

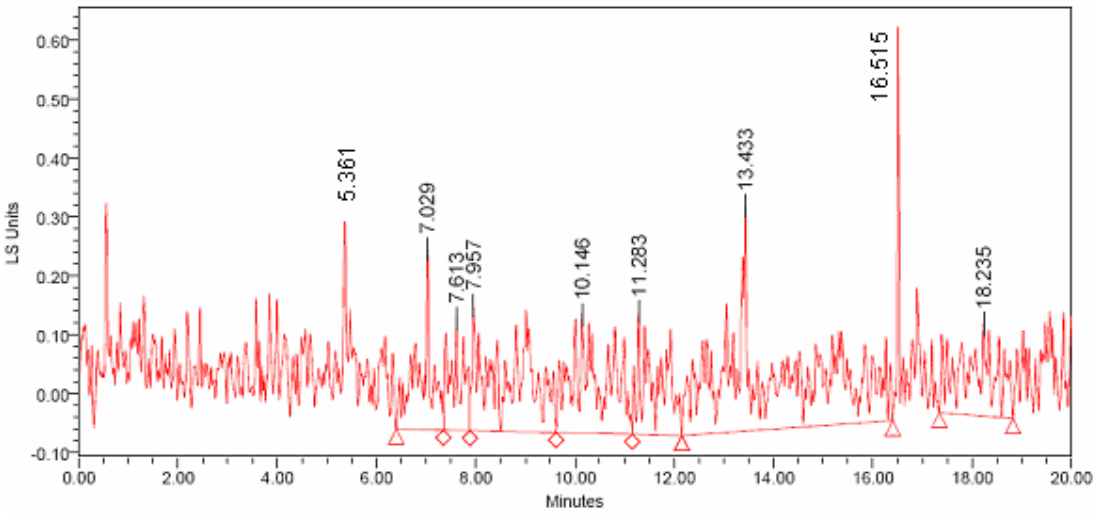

Figure 4.14. Chromatogram of BY743 grown in YPD

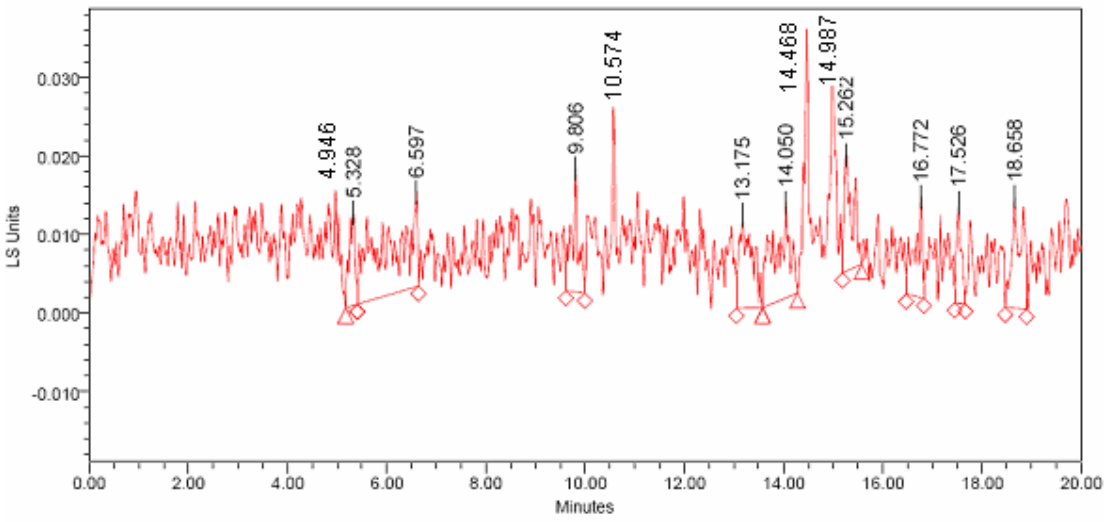

Figure 4.15. Chromatogram of BY743 grown in F1

Table 4.15. Summary of sphingolipid profiles of BY4743 grown in YPD

Peaks	Retention Time (min)	Area (µVxsec)	Standard Matched	Experimental Concentration (mM)	Possible Compound
1	5.361	2077	C8-Cer	0.048562076	IPC
2	7.029	4480	PHS	0.002978713	PHS
3	7.613	2991			
4	7.957	9467	P-Cer	0.003466788	P-Cer
5	10.146	8405	C2-Cer	4.90646E-05	DHS-P
6	11.283	5198			
7	13.433	21959		0.009209631	MIPC
8	16.515	4994		0.000472222	$M(IP)_2C$
9	18.235	6490		0.001996465	D-Cer

When Figure 4.14 and Figure 4.15 were investigated, it was seen that with YPD medium, the heights of the peaks were in the range of 10^{-1} while peak heights with F1 medium were in the 10^{-2} range. This means that sphingolipid amounts differed by 10 fold with the medium change even if the strain under consideration was the same one. Possible reasons for this result was the fact that in YPD, unlimited medium, the compounds other than glucose were in higher concentrations than that in F1, minimal medium. This

difference was more clearly seen from the peak and area summaries of the chromatograms for both media given in Table 4.15 and Table 4.16.

When the tables were analyzed, beside the difference among the peak height and corresponding area magnitudes, some additional peaks were present in the chromatogram of the wild type strain grown in F1. Possible reason for this observation might be again the differences in the initial concentrations of the nutrients in the media. The low initial concentrations in F1 medium were limiting the sphingolipid production so that intermediate sphingolipids were seen on the profile of BY4743.

For wild type strain grown in F1 medium, a slight increase in P-Cer/PHS value was observed along with a decrease in DHS-P/PHS value (Table 4.17). So, DHS, instead of being converted to DHS-P, tended to shift to the production of PHS, which in turn, proceeded with the synthesis of P-Cer.

Table 4.16. Summary of sphingolipid profiles of BY4743 grown in F1

Peaks	**Retention Time (min)**	**Area (μVxsec)**	**Standard Matched**	**Experimental Concentration (mM)**	**Possible Compound**
1	4.964	101	C8-Cer	0.002361468	IPC
2	5.328	99	PHS	0.000084405	PHS
3	6.597	449	P-Cer	0.000305195	P-Cer
4	9.806	140			
5	10.574	120	C2-Cer	0.000000703	DHS-P
6	13.175	208		0.000087235	MIPC
7	14.05	254			
8	14.468	306			
9	14.987	248	C18-DHS	0.000085495	DHS
10	15.262	169			
11	16.772	129		0.000012198	$M(IP)_2C$
12	17.526	83			
13	18.658	190		0.000058448	D-Cer

Table 4.17. Comparison of experimental data with literature for BY4743 grown in F1

	Proportions in Literature for BY4743 in YPD	**Experimental Proportions for BY4743 in F1**
D-Cer/PHS	0.798	0.692
DHS-P/PHS	0.020	0.008
P-Cer/PHS	1.054	3.616
IPC/PHS	22.938	27.978
MIPC/PHS	2.799	1.034
$M(IP)_2C$/PHS	0.170	0.145

4.4.3. Sphingolipid Qualification and Quantification for *INO1*

ino1Δ/ino1Δ homozygous mutant was grown in YPD, F1 and F1 without inositol media to see the effects of inositol transport from medium into the cell, while *INO1/ino1Δ* heterozygous mutant was grown in YPD medium only.

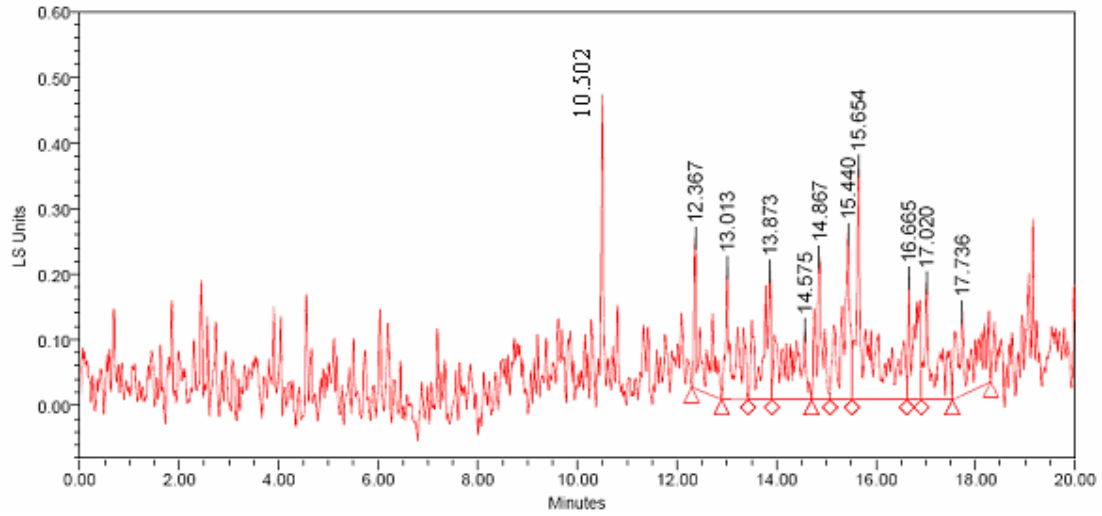

Figure 4.18. Chromatogram of *ino1Δ/ino1Δ* mutant grown in YPD

When Figure 4.18 and 4.19 were compared, it was seen that sphingolipid profile of both *INO1/ino1Δ* mutant and *ino1Δ/ino1Δ* mutant were in the same range with that of the wild type, BY4743. This was an expected result, since these mutant strains were grown in

rich medium, YPD. However, the main difference between the homozygous and heterozygous mutant strains was the accumulation of peaks at later retention time values in homozygous strain. The main reason for this attitude might be the limitation of inositol containing sphingolipid synthesis in *ino1Δ/ino1Δ* due to the lack of the inositol 1-phosphate synthase in the mutant. Although the cells could have incorporated inositol present in the medium, the mechanism was somehow disrupted and the peaks of higher intensities after 10 min were probably corresponding to some intermediate sphingolipids, or even to some phospholipids which were not shown on Figure 2.1, produced in the previous steps of CDP-E synthesis.

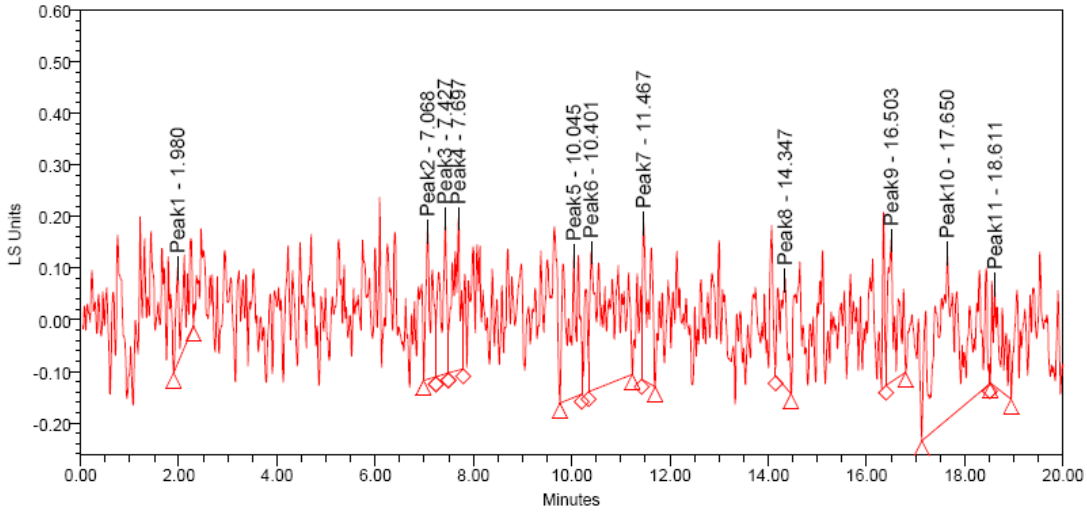

Figure 4.19. Chromatogram of *INO1/ino1Δ* mutant grown in YPD

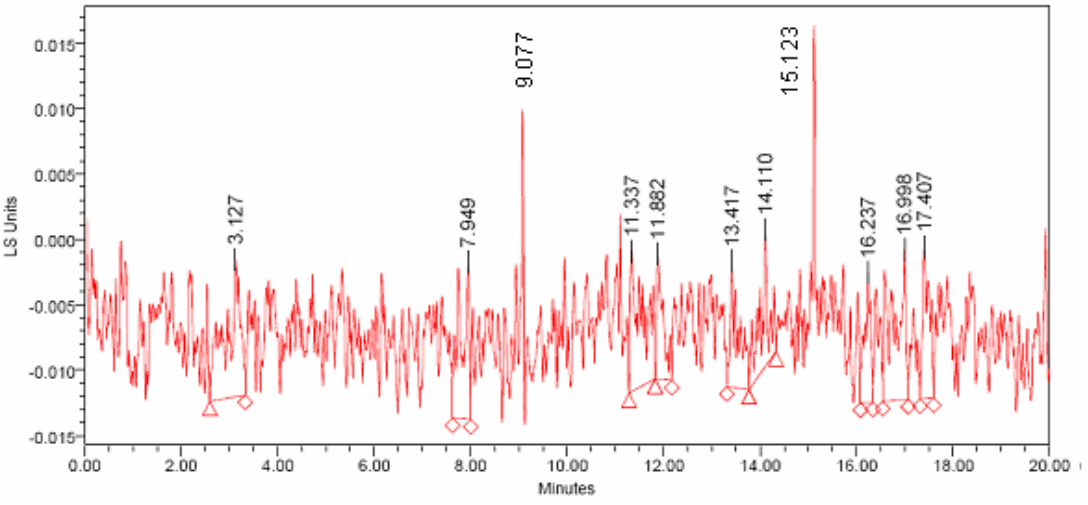

Figure 4.20. Chromatogram of *ino1Δ/ino1Δ* mutant grown in F1

However, it was seen that with YPD medium, the heights of the peaks were in the range of 10^{-1} while peak heights with F1 medium were in the 10^{-2} range. This means that sphingolipid amount diminished dramatically with the medium change even if the strain under consideration was the same one. Possible reasons for this result was again the rich nutrients in YPD, unlimited medium, compared to those in F1, minimal medium.

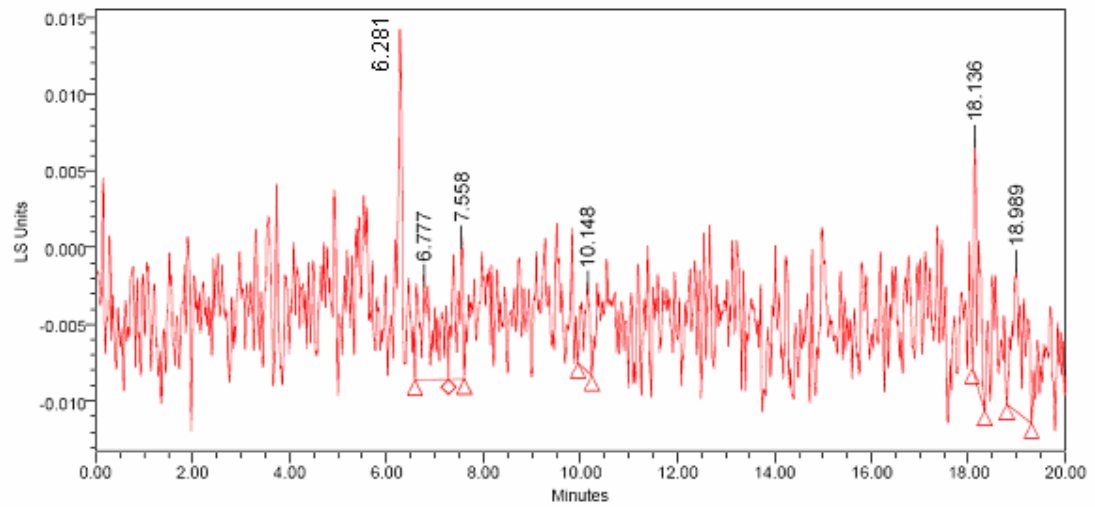

Figure 4.21. Chromatogram of *ino1Δ/ino1Δ* mutant grown in F1 without inositol

Table 4.18. Summary of sphingolipids of *ino1Δ/ino1Δ* mutant grown in YPD

Peaks	**Retention Time (min)**	**Area (μVxsec)**	**Standard Matched**	**Experimental Concentration (mM)**	**Possible Compound**
1	10.502	1169	C2-Cer	0.000006843	DHS-P
2	12.367	2003			
3	13.873	4264		0.001788327	MIPC
4	14.575	2665	C-18 DHS	0.000720121	DHS
5	14.867	1770			
6	15.44	2651			
7	15.654	4988			
8	16.665	1784		0.000168691	$M(IP)_2C$
9	17.02	2071			
10	17.736	2630			

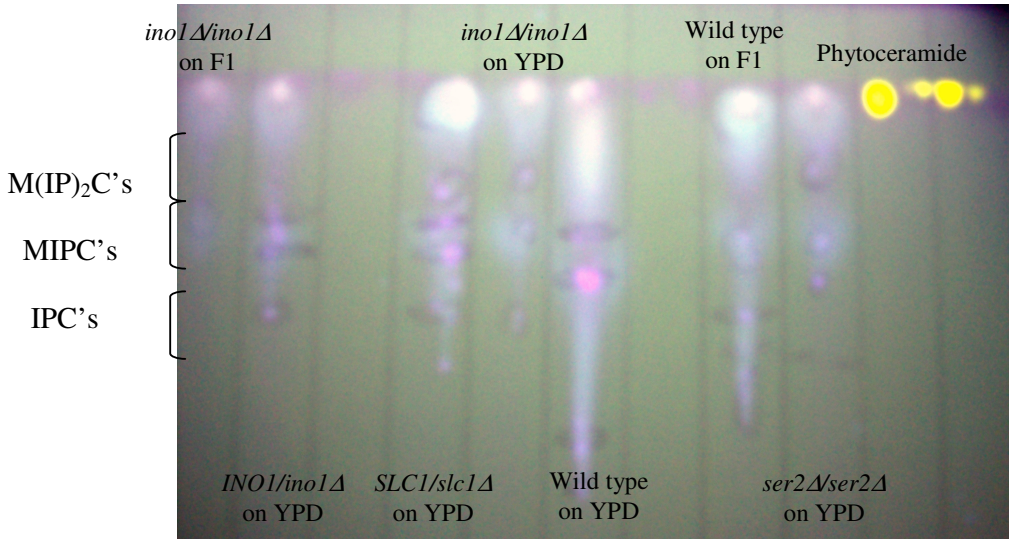

Figure 4.22. TLC analysis of wild type and mutant strains sphingolipids

Profile of *ino1Δ/ino1Δ* mutant grown in YPD and F1 media, presented an interesting feature, MIPC and also $M(IP)_2C$ were present in the chromatograms. It was an unexpected result, since the strain lacked inositol synthase enzyme, it could not produce sphingolipids containing inositol. When this effect was seen, it was suspected that the retention time values attibuted to MIPC and $M(IP)_2C$ were not correct. However, a TLC analysis confirmed that the strain grown in YPD and F1 media indeed produced MIPC and $M(IP)_2C$, and this was not an annotation problem (Figure 4.22).

Table 4.19. Summary of sphingolipids of *ino1Δ/ino1Δ* mutant grown in F1 without inositol

Peaks	Retention Time (min)	Area (μVxsec)	Standard Matched	Experimental Concentration (mM)	Possible Compound
1	6.281	202	PHS	0.000171329	PHS
2	6.777	146	P-Cer	0.000100778	P-Cer
3	7.558	94			
4	10.148	56	C2-Cer	0.000000328	DHS-P
5	18.136	96			
6	18.989	156	D-Cer	0.000047989	D-Cer

So, even the homozygous strain produced MIPC and $M(IP)_2C$, incorporating the inositol present in the medium. That is the reason why an F1 medium without inositol was also prepared to be used as medium for growth of *ino1Δ/ino1Δ* mutant. The results for this setup were given in Table 4.19.

Table 4.20. Summary of sphingolipids of *INO1/ino1Δ* mutant grown in YPD

Peaks	**Retention Time (min)**	**Area (μVxsec)**	**Standard Matched**	**Experimental Concentration (mM)**	**Possible Compound**
1	1.98	2381			
2	7.068	2287	PHS	0.001735471	PHS
3	7.427	2439			
4	7.697	2941	P-Cer	0.001744261	P-Cer
5	10.045	4290	C2-Cer	0.000025082	DHS-P
6	10.401	8287			
7	11.467	2858			
8	14.347	2294	C18-DHS	0.000646113	DHS
9	16.503	3085		0.001293853	$M(IP)_2C$
10	17.65	12816			
11	18.611	2548			

When *ino1Δ/ino1Δ* mutants' profiles for growth media of F1 and F1 without inositol given in Table 4.19 and Table 4.21 were investigated, it was seen that beside the absence of inositol containing sphingolipids in *ino1Δ/ino1Δ* mutant grown in F1 without inositol, an increase in intermediate ceramides, D-Cer and P-Cer was observed. Dry weight/ l value for *ino1Δ/ino1Δ* mutant grown in F1 without inositol was much lower than that grown in F1 containing inositol, so it was speculated that P-Cer and/or D-Cer were apoptotic sphingolipids.

In the homozygous deletion mutant strains, grown in YPD and F1 media, both complex sphingolipids, MIPC and $M(IP)_2C$ were detectable while in *INO1/ino1Δ* mutant only the end ceramide, $M(IP)_2C$ was observed. Since the gene was deleted from both of the

alleles in the homozygous mutant strain, the inositol containing ceramides were produced upon the transported inositol from the medium. But for the heterozygous mutant, both the incorporation and synthesis of inositol occurred, which was less limiting for the synthesis of complex sphingolipids, that might be the reason why $M(IP)_2C$, the ultimate complex sphingolipid was dominant in its profile.

Table 4.21. Summary of sphingolipids of *ino1Δ/ino1Δ* mutant grown in F1

Peaks	**Retention Time (min)**	**Area (μVxsec)**	**Standard Matched**	**Experimental Concentration (mM)**	**Possible Compound**
1	3.127	212			
2	7.949	143	P-Cer	0.000098722	P-Cer
3	9.077	157	C2-Cer	0.000000919	DHS-P
4	11.337	184			
5	11.882	85			
6	13.417	108		0.000045295	MIPC
7	14.11	115			
8	15.123	275	C18-DHS	0.000094574	DHS
9	16.237	85			
10	16.998	195		0.000018439	$M(IP)_2C$
11	17.407	110			

Table 4.22. Comparison of experimental data of *ino1Δ/ino1Δ* mutant in YPD with that of BY4743

	Proportions in Literature for BY4743 in YPD	**Experimental Proportions for *ino1Δ/ino1Δ* in YPD**
DHS-P/DHS	0.100	0.010
MIPC/DHS	14.002	2.483
$M(IP)_2C$/DHS	0.850	0.234

Table 4.23. Comparison of experimental data of *INO1/ino1Δ* mutant in YPD with that of BY4743 in YPD

	Proportions in Literature for BY4743 in YPD	**Experimental Proportions for *INO1/ino1Δ* in YPD**
DHS-P/DHS	0.100	0.039
PHS/DHS	5.003	2.686
$M(IP)_2C$/DHS	0.850	2.003
P-Cer/DHS	5.271	2.700

Table 4.24. Comparison of experimental data of *ino1Δ/ino1Δ* mutant in F1 without inositol with that of BY4743 in F1

	Proportions for BY4743 in F1	**Experimental Proportions for *ino1Δ/ino1Δ* in F1 without inositol**
D-Cer/PHS	0.692	0.280
DHS-P/PHS	0.008	0.002
P-Cer/PHS	3.616	0.588

Table 4.25. Comparison of experimental data of *ino1Δ/ino1Δ* mutant in F1 with data of BY4743 in F1

	Proportions for BY4743 in F1	**Experimental Proportions for *ino1Δ/ino1Δ* in F1**
DHS-P/DHS	0.008	0.010
MIPC/DHS	1.020	0.479
$M(IP)_2C$/DHS	0.143	0.195
P-Cer/DHS	3.570	1.044

The profiles of *ino1Δ/ino1Δ* mutants grown in F1 and F1 without inositol, differed also in sphingoid base content. For the mutant grown in F1, the sphingoid base observed was DHS, while for F1 without inositol, it was PHS. As it could be seen from Table 4.24, for the mutant grown in F1 medium without inositol only, the presence of D-Cer was detected. This might suggest that DHS in this mutant strain was converted to D-Cer preferably, avoiding accumulation in the limits of detection.

4.4.4. Sphingolipid Qualification and Quantification for *SLC1*

SLC1/slc1Δ mutant was grown in YPD while *slc1Δ/slc1Δ* mutant was grown in both YPD and F1 media. When chromatograms of these strains grown in different media were investigated, it was seen that *SLC1/slc1Δ* mutant's sphingolipid profile resembled to that of the BY4743 profile in range (Figure 4.23). Although the individual amounts of shared sphingolipids were lower in *SLC1/slc1Δ* than wild type strain, both grown in YPD, which was exceptable.

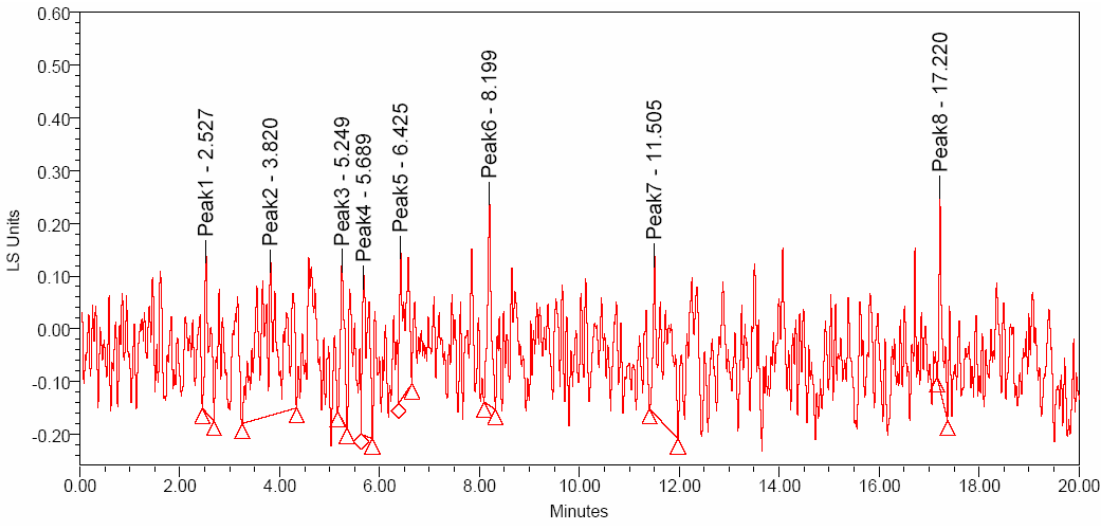

Figure 4.23. Chromatogram of *SLC1/slc1Δ* mutant grown in YPD

But interestingly, *slc1Δ/slc1Δ* mutant grown in YPD exhibited a different property, the amount of some sphingolipids, especially PHS, DHS and DHS-P, were higher than those in wild type, which can be seen from the area values given in Table 4.28. The same

fact was also seen when wild type strain was compared with *slc1Δ/slc1Δ* mutant grown in F1, still amounts of PHS and DHS were remarkably higher (Table 4.26 and Table 4.16).

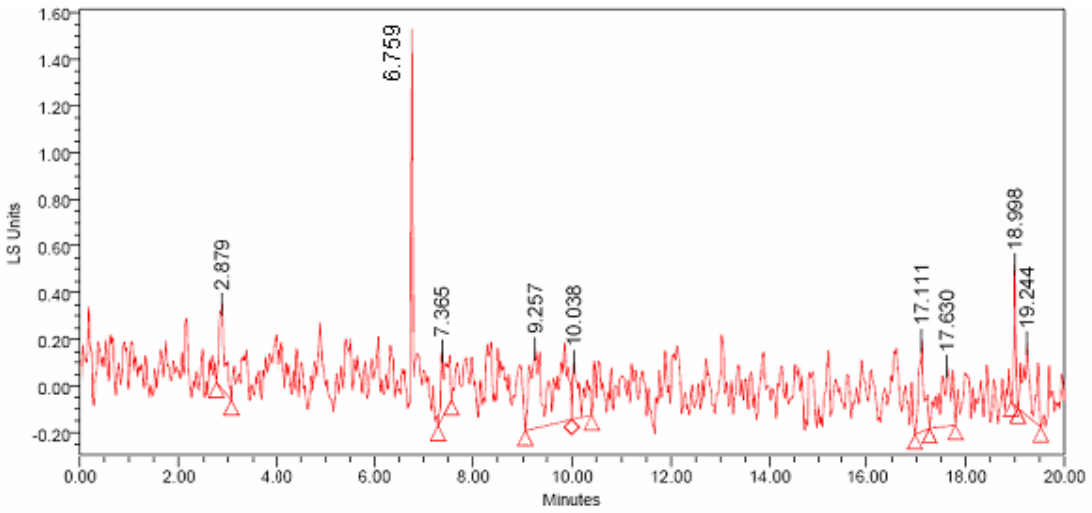

Figure 4.24. Chromatogram of *slc1Δ/slc1Δ* mutant grown in YPD

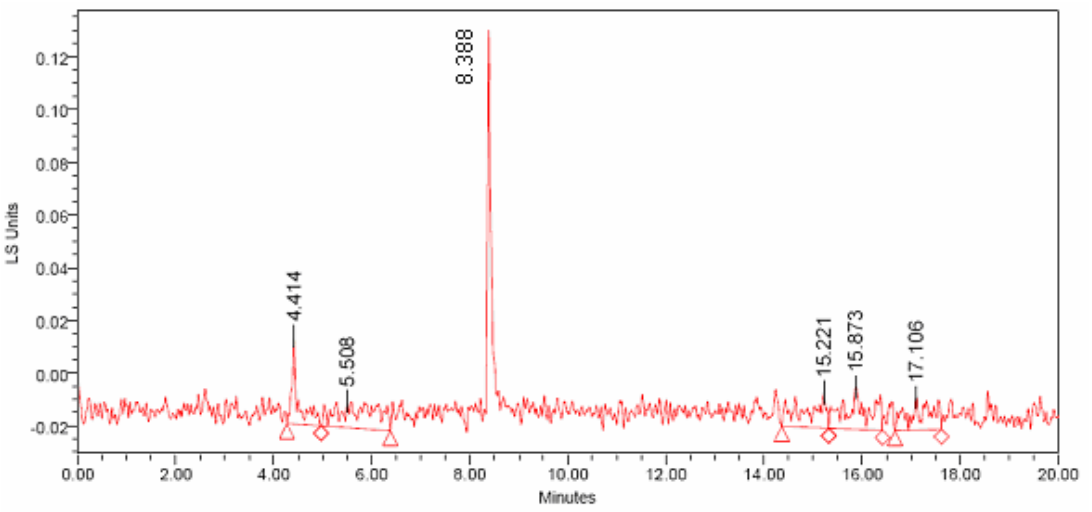

Figure 4.25. Chromatogram of *slc1Δ/slc1Δ* mutant grown in F1

SLC1 encodes a putative sn-2 specific acyltransferase. *SLC1* was first recognized as a 1-acylglycerol-3-phosphate O-acyltransferase in a screen for second site suppressor mutations that would allow yeast to grow in the absence of sphingolipids (Benghezal *et al.*, 2007). Furthermore, it was reported that in *SLC1* deletion mutants, the total amounts of PI's, PS2s and PE's diminished about 60 per cent (Benghezal *et al.*, 2007). One may suggest that for *slc1Δ/slc1Δ* mutant the synthesis was shifted towards the sphingoid base

production rather than phospholipid production which supported previously mentioned findings. For *SLC1/slc1Δ* mutant however, this effect was not seen, meaning that heterozygosity balanced the production, in a fashion similar to the wild type strain.

Although the amounts of all the sphingolipids seen in the chromatogram of *slc1Δ/slc1Δ* mutant grown in F1 medium were higher than the ones of wild type strain grown in F1 medium, their proportions to PHS, as given in Table 4.27 were lower than in the wild type case. Since PHS amount was increased about five fold while the increase in the other species was relatively very low, overall proportions were found to be decreased.

Table 4.26. Summary of sphingolipids of *slc1Δ/slc1Δ* mutant grown in F1

Peaks	**Retention Time (min)**	**Area (μVxsec)**	**Standard Matched**	**Experimental Concentration (mM)**	**Possible Compound**
1	4.414	293			
2	5.508	527	PHS	0.000439645	PHS
3	8.388	781	P-Cer	0.000521849	P-Cer
4	15.221	359	C18-DHS	0.000122533	DHS
5	15.873	486		0.000045955	$M(IP)_2C$
6	17.106	358		0.000008523	

Table 4.27. Comparison of experimental data of *slc1Δ/slc1Δ* mutant in F1 with data for BY4743 in F1

	Proportions in Literature for BY4743 in F1	**Experimental Proportions for *slc1Δ/slc1Δ* in F1**
DHS/PHS	1.013	0.279
P-Cer/PHS	3.616	1.187
$M(IP)_2C$/PHS	1.034	0.105

The same behaviour was observed for *slc1Δ/slc1Δ* mutant grown in YPD. Again, individual sphingoid base species such as PHS and DHS-P were in higher amounts in the

mutant strain than those in the wild type, but the overall proportions were decreased (Table 4.29).

Table 4.28. Summary of sphingolipids of *slc1Δ/slc1Δ* mutant grown in YPD

Peaks	**Retention Time (min)**	**Area (μVxsec)**	**Standard Matched**	**Experimental Concentration (mM)**	**Possible Compound**
1	2.879	2816			
2	6.759	8271	PHS	0.004156023	PHS
3	7.365	2627	P-Cer	0.001586710	P-Cer
4	9.257	10658	C2-Cer	0.000062164	DHS-P
5	10.038	2901			
6	17.111	2948		0.000278757	$M(IP)_2C$
7	17.63	4365			
8	18.998	1547		0.000475891	D-cer
9	19.224	3812			

Table 4.29. Comparison of experimental data of *slc1Δ/slc1Δ* mutant in YPD with that of BY4743 in YPD

	Proportions in Literature for BY4743 in YPD	**Experimental Proportions for *slc1Δ/slc1Δ* in YPD**
D-Cer/PHS	0.798	0.115
DHS-P/PHS	0.020	0.015
P-Cer/PHS	1.054	0.382
$M(IP)_2C$/PHS	14.909	0.067

For heterozygous *SLC1/slc1Δ* mutant grown in YPD, IPC was detected in the sphingolipid profile whereas $M(IP)_2C$ was encountered in the profile of homozygous *slc1Δ/slc1Δ* mutant independent of the medium. The reason for this difference may be that the gene deletion might have shifted the sphingolipid synthesis mechanism towards the complex ceramide production, not to the sphingoid base production. In the homozygous

strain, since genes on both of the alleles were deleted, the intermediate complex ceramides, IPC and MIPC were not even seen on the chromatogram but the end product, $M(IP)_2C$. The heterozygous strain exhibited similar features with the wild type strain for the proportions (Table 4.31).

Table 4.30. Summary of sphingolipids of *SLC1/slc1Δ* mutant grown in YPD

Peaks	Retention Time (min)	Area (μVxsec)	Standard Matched	Experimental Concentration (mM)	Possible Compound
1	2.527	1879			
2	3.82	8876			
3	5.249	1658	C8-Cer	0.038765490	IPC
4	5.689	2538	PHS	0.001898648	PHS
5	6.425	2665			
6	8.199	2033	P-Cer	0.001269918	P-Cer
7	11.505	5002			
8	17.22	1619			

Table 4.31. Comparison of experimental data of *SLC1/slc1Δ* mutant in YPD with that of BY4743 in YPD

	Proportions in Literature for BY4743 in YPD	Experimental Proportions for *SLC1Δ/slc1Δ* in YPD
P-Cer/PHS	1.054	0.669
IPC/PHS	22.938	20.417

4.4.5. Sphingolipid Qualification and Quantification for *SER2*

ser2Δ/ser2Δ mutant was grown in YPD and F1 media. However, as indicated by its name, serine requiring mutant was not able to grow in F1 medium. The sphingolipid chromatogram of *ser2Δ/ser2Δ* mutant was given in Figure 4.26.

Table 4.32. Summary of sphingolipids of *ser2Δ/ser2Δ* mutant grown in YPD

Peaks	Retention Time (min)	Area (μVxsec)	Standard Matched	Experimental Concentration (mM)	Possible Compound
1	2.057	2340			
2	2.204	2555			
3	2.899	3121			
4	3.137	3877			
5	3.908	8331			
6	4.369	1905	C20-DHS	0.000072035	not known
7	5.066	8096	C8-Cer	0.189291560	IPC
8	7.253	1826	PHS	0.001421708	PHS
9	8.429	12708	P-Cer	0.003221712	P-Cer
10	9.167	2820			
11	9.311	3102			
12	9.869	10378	C2-Cer	0.000060537	DHS-P
13	10.72	1833			
14	11.431	9258			
15	12.449	9875		0.004141587	MIPC
16	13.294	4306			
17	13.752	435			
18	14.229	3102	C18-DHS	0.000796407	DHS

When the chromatogram of *ser2Δ/ser2Δ* mutant grown in YPD was investigated, it was seen that it was similar in range to that of the wild type strain. However, an increase in especially intermediate ceramides such as IPC and P-cer was observed in this mutant. Actually it was expected that this strain would be unable to produce any sphingolipids at all, since the gene encoding the enzyme catalyzing serine production at the very begining of the sphingolipid mechanism was deleted, but since serine was available in the medium, its incorporation rendered the cells capable of producing sphingolipids as can be seen on Table 4.32.

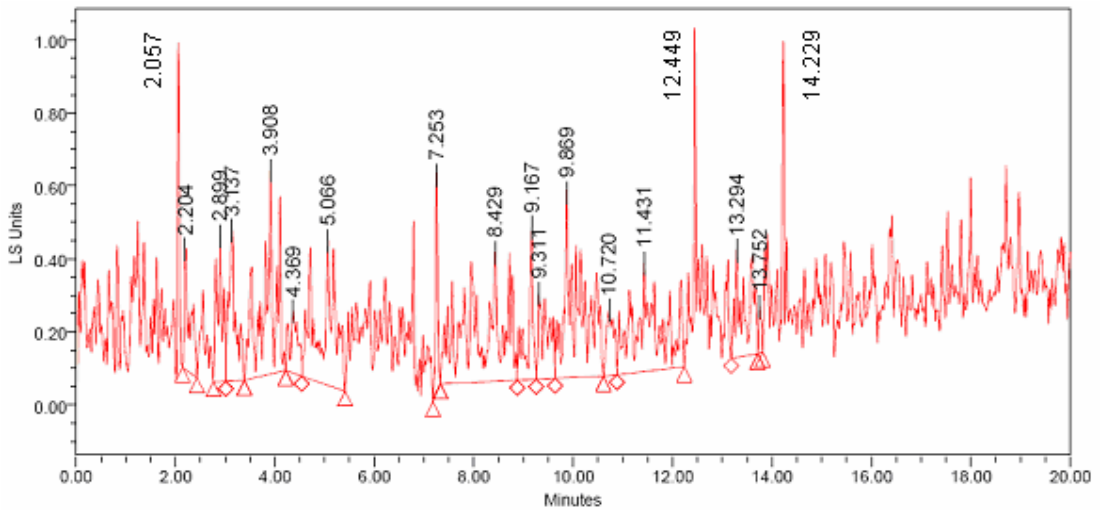

Figure 4.26. Chromatogram of *ser2Δ/ser2Δ* mutant grown in YPD

When the sphingolipid summary of *ser2Δ/ser2Δ* mutant given in Table 4.32 was compared to that of the wild type summary, it was seen that sphingolipid proportions for this strain were higher than the ones of the wild type. The main reason for this was that the PHS amount in the mutant strain was lower than that in wild type and since PHS was on the denominator, the proportions were increased in the homozygous strain.

The main difference between the sphingolipid profiles of *ser2Δ/ser2Δ* mutant and BY4743 was the increase in P-Cer and IPC amounts in *ser2Δ/ser2Δ* mutant and the presence of a previously unseen standard match, C20-DHS. In the sphingolipid synthesis mechanism of yeast, Lcb1p and Lcb2p catalyze the production of KDHS, by using serine the production of which is catalyzed by Ser2p. This is the first and committed step in the sphingolipid synthesis. So, it was logical to conclude that *ser2Δ/ser2Δ* mutant grown in YPD, should generate a similar sphingolipid profile with *LCB1* and/or *LCB2* deletion mutants. Indeed, sphingolipid profile summary of *LCB1/ lcb1Δ* mutant given in Table 4.35 was quite similar to that one of the *ser2Δ/ser2Δ* mutant's summary, it had C20-DHS too, which was suspected to be a phospholipid compound. Also, *LCB1* and *LCB2* homozygous mutants were reported to be inviable (Buede et al., 1991), so by analogy, it can be speculated that *ser2Δ/ser2Δ* mutant, with elevated P-Cer levels mimicked this attitude since P-Cer in yeast was thought to lead to apoptosis. Although it was viable with the exogeneous serine transport it had the lowest biomass value of 4.42 g/l among all the strains grown in YPD.

Table 4.33. Comparison of experimental data of *ser2Δ/ser2Δ* mutant in YPD with that of BY4743 in YPD

	Proportions in Literature for BY4743 in YPD	**Experimental Proportions for *ser2Δ/ser2Δ* in YPD**
DHS/PHS	0.200	0.560
DHS-P/PHS	0.020	0.043
P-Cer/PHS	1.054	2.266
IPC/PHS	22.938	133.144
MIPC/PHS	2.799	2.913

4.4.6. Sphingolipid Qualification and Quantification for *LCB1* and *LCB2*

LCB1/lcb1Δ and *LCB2/lcb2Δ* were grown in YPD medium. Since the homozygous diploid strains have been reported to be inviable, heterozygous mutant strains were used in this study. Their respective chromatograms were given in Figure 4.27 and 4.28.

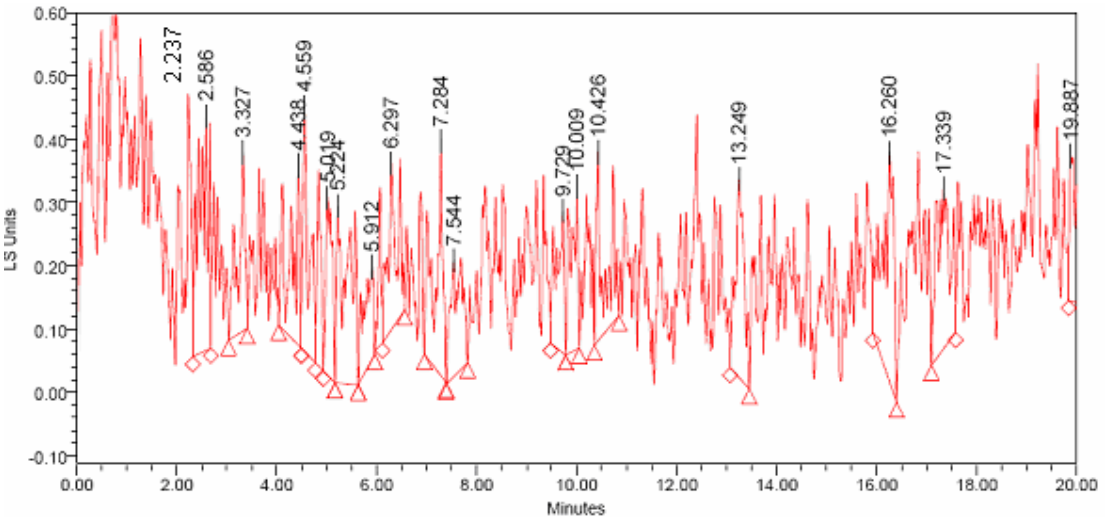

Figure 4.27. Chromatogram of *LCB1/lcb1Δ* mutant grown in YPD

The sphingolipid amounts in both of the mutants were in the same range with wild type sphingolipid amounts, 10^{-1}. However, *LCB1/lcb1Δ* mutant shared a similar profile

with wild type strain grown in YPD, even it had more peaks at lower retention time values while *LCB2/lcb2Δ* lacked many of the peaks that wild type strain and *LCB1/lcb1Δ* possessed, as could be seen from Table 4.34, Table 4.35 and Table 4.14.

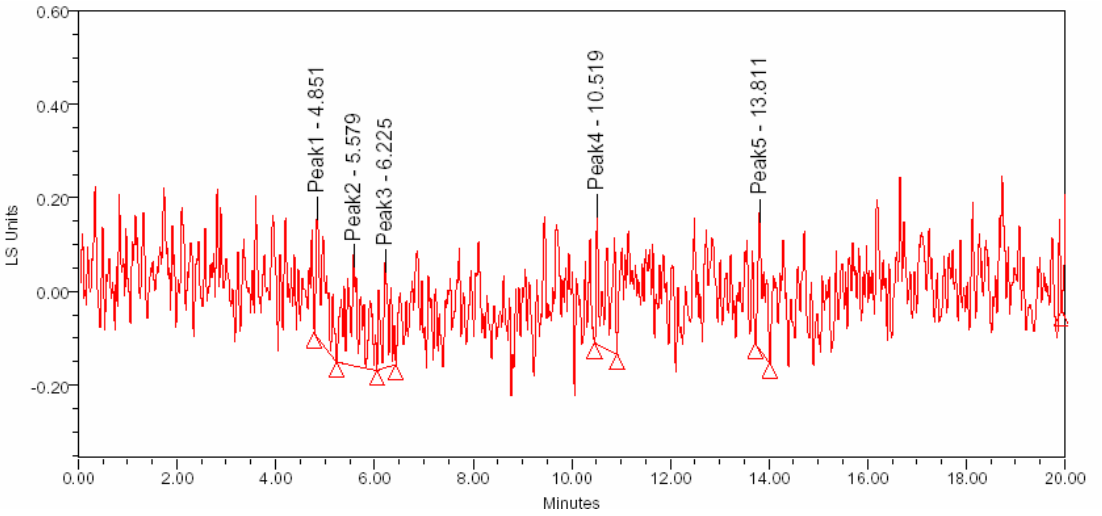

Figure 4.28. Chromatogram of *LCB2/lcb2Δ* mutant grown in YPD

Table 4.34. Summary of sphingolipids of *LCB2/lcb2Δ* mutant grown in YPD

Peaks	Retention Time (min)	Area (µVxsec)	Standard Matched	Experimental Concentration (mM)	Possible Compound
1	4.851	3157			
2	5.579	4879	C8-Cer	0.114075286	IPC
3	6.225	2162	PHS	0.001652193	PHS
4	10.519	3435	C2-Cer	0.000020089	DHS-P
5	13.811	2446		0.001025855	MIPC

The *LCB1* and *LCB2* genes, found to be required for SPT activity using genetic screens in *Saccharomyces cerevisiae*, encode proteins homologous to the α–oxoamine synthases that all catalyze the condensation of a carboxylic acid CoA thioester with the α-carbon of an amino acid. Homologs of the *LCB1* and *LCB2* genes from higher eukaryotes have been identified based on their similarity to the *S. cerevisiae LCB* genes. It was revealed that several functionally important residues, are highly conserved in the α-

oxoamine synthases. Although Lcb1p and Lcb2p are homologous to each other and to α-oxoamine synthases, many of these conserved residues are present in Lcb2p, but not in Lcb1p (Gable *et al.*, 2002).

Table 4.35. Summary of sphingolipids of *LCB1/lcb1Δ* mutant grown in YPD

Peaks	Retention Time (min)	Area (μVxsec)	Standard Matched	Experimental Concentration (mM)	Possible Compound
1	2.237	2555			
2	2.586	5103			
3	3.327	2606			
4	4.438	3174	C20-DHS	0.000179691	not known
5	4.559	3127			
6	5.019	2440	C6-Cer	0.000015416	not known
7	5.224	4774	C8-Cer	0.111620295	IPC
8	5.912	2006			
9	6.297	3307	PHS	0.002364980	PHS
10	7.284	3961	P-Cer	0.002208742	P-Cer
11	7.544	2948			
12	9.729	2440			
13	10.009	2571			
14	10.426	3080	C2-Cer	0.000018016	DHS-P
15	13.249	3800		0.001593724	MIPC
16	16.26	5360		0.000000002	$M(IP)_2C$
17	17.339	4812			
18	19.887	2503			

The sphingolipid amounts and types produced by *LCB1/lcb1Δ* mutant were similar to wild type, the effect of the heterozygosity was on the production of new and unseen peaks in the chromatogram of the wild type strain. These peaks might be intermediate sphingolipids which were not produced in a significant amount in BY4743, so they were not present in its chromatogram. Another interesting feature of *LCB1/lcb1Δ* mutant's

chromatogram was the similarity it possessed with *ser2Δ/ser2Δ* mutant's chromatogram (Table 4.35 and Table 4.32). Since Lcb1p and Ser2p were working in parallel as could be seen on Figure 2.1, their mutations yielded similar results.

Table 4.36. Comparison of experimental data of *LCB1/lcb1Δ* mutant in YPD with that of BY4743 in YPD

	Proportions in Literature for BY4743 in YPD	**Experimental Proportions for *LCB1/lcb1Δ* grown in YPD**
DHS-P/PHS	0.020	0.008
P-Cer/PHS	1.054	0.934
IPC/PHS	22.938	47.197
MIPC/PHS	2.799	0.674
$M(IP)_2C$/PHS	0.170	0.214

The heterozygous deletion of *LCB2* affected the sphingolipid production dramatically, especially when compared to the heterozygous deletion of *LCB1*. One reason for this effect might be the relative "essentiality" of *LCB2* compared to *LCB1*, with the functionally important residues highly conserved in its structure (Gable *et al.*, 2002).

Table 4.37. Comparison of experimental data of *LCB2/lcb2Δ* mutant in YPD with that of BY4743 in YPD

	Proportions in Literature for BY4743 in YPD	**Experimental Proportions for *LCB2/lcb2Δ* grown in YPD**
DHS-P/PHS	0.020	0.012
IPC/PHS	22.938	69.045
MIPC/PHS	2.799	0.621

When the proportions were observed, an increase in IPC over PHS values for both of the heterozygous mutants was observed, in contrast to the decrease in other proportions (Table 4.36 and Table 4.37). The decrease in the proportions of other sphingolipids was expected, since the genes at the very beginning of the sphingolipid synthesis mechanism were deleted. The presence of D-Cer in wild type profile but not in *LCB1/lcb1Δ* nor in *LCB2/lcb2Δ* might explain this situation. D-Cer, instead of accumulating in the heterozygous mutants, might have been converted to IPC.

5. CONCLUSIONS AND RECOMMENDATIONS

5.1. Conclusions

In this study, BY4743 parent strain and its five deletion mutants of genes *INO1*, *SLC1*, *SER2*, *LCB1*, and *LCB2* of the yeast *Saccharomyces cerevisiae* were investigated to improve present knowledge on the sphingolipid synthesis mechanism and to qualify as well as to quantify sphingolipids in yeast by HPLC.

For this purpose, cells were grown in rich medium, YPD, in batch cultivations and the wild type along with homozygous deletions mutants was also cultivated in limited/minimal medium, F1. Lipid extraction method to be used was determined via TLC. The extracted lipids were loaded to HPLC for the qualification and quantification process for each strain. For qualification and quantification processes, various sphingolipid standards were injected to HPLC in different concentrations to obtain a calibration curve for each standard. The retention time resemblance with these standards was the basis for qualification, whereas for the quantification process calibration curves were used.

Sphingolipid profile of wild type strain matched well with the profile given in literature, both for F1 and YPD media adopted. The effect of the medium was seen on the amounts produced, in F1 medium sphingolipid production decreased by approximately 10 fold with respect to YPD medium. This would be expected since YPD was a rich medium, while F1 was a limiting one.

In *ino1Δ/ino1Δ* mutant's profile in F1 without inositol, beside the absence of inositol containing sphingolipids, an increase in intermediate ceramides, D-Cer and P-Cer was observed. This effect was not seen from Table 5.1, since in the homozygous mutant strain, PHS level was also increased with respect to BY4743 strain grown in F1. Dry weight/l value for *ino1Δ/ino1Δ* mutant grown in F1 without inositol was much lower than that grown in F1 and YPD, so it was speculated that P-Cer and/or D-Cer might be apoptotic sphingolipids as stated in the literature. In the homozygous deletion mutant strains, grown

in YPD and F1 media, both complex sphingolipids, MIPC and $M(IP)_2C$ were detectable while in heterozygous *INO1/ino1Δ* mutant only the end ceramide, $M(IP)_2C$ was observed.

For *slc1Δ/slc1Δ* mutant grown in YPD and F1 media the amount of some sphingolipids, especially PHS and DHS or DHS-P were higher than those in wild type. On Table 5.1, the fact that P-Cer over PHS values diminished was quite clear whereas increase in sphingoid bases was not easily distinguished due to the fact that PHS was in the denominator. This homozygous mutant strain had also overgrown the wild type. PHS and/or DHS were reported to be growth stimulating sphingolipids in literature, these results might support this knowledge. For *SLC1/slc1Δ* mutant however, this effect was not seen, meaning that heterozygosity balanced the production, in a fashion similar to the wild type strain.

The main difference between the sphingolipid profiles of *ser2Δ/ser2Δ* mutant and BY4743 was the increase in P-Cer and IPC amounts in *ser2Δ/ser2Δ* mutant's chromatogram (Table 5.1) and the presence of a previously unseen standard match, C20-DHS. C20-DHS was also seen in the sphingolipid profile of *LCB1/ lcb1Δ* mutant, and was suspected to be a phospholipid compound. Also, *ser2Δ/ser2Δ* mutant had the lowest dry weight/l value among the strains grown in YPD, in aggrement with the suspicion that P-Cer is an apoptotic sphingolipid in yeast.

The sphingolipid amounts and types produced by *LCB1/lcb1Δ* mutant were similar to wild type, the effect of the heterozygosity was on the production of new and unseen peaks in the chromatogram of the wild type strain. The heterozygous deletion of *LCB2* affected the sphingolipid production dramatically, its chromatogram had approximately one third of the sphingolipid compounds present in *LCB1/lcb1Δ* mutant's chromatogram. When the proportions of some major sphingolipids were calculated, an increase in IPC over PHS values for both of the heterozygous mutants was observed, in contrast to the decrease in other proportions. The presence of D-Cer in wild type profile but not in *LCB1/lcb1Δ* and *LCB2/lcb2Δ* mutants might explain this situation. D-Cer, instead of accumulating in the heterozygous mutants, might have been converted to IPC (Table 5.1).

Table 5.1. Summary of sphingolipid proportions of different strains

	DHS/PHS	**D-Cer/PHS**	**DHS-P/PHS**	**P-Cer/PHS**
BY4743 in YPD	0.200	0.798	0.020	1.054
INO1/ino1Δ in YPD	0.372		0.014	1.005
ser2Δ/ser2Δ in YPD	0.560		0.043	2.266
LCB1/lcb1Δ in YPD			0.008	0.934
LCB2/lcb2Δ in YPD			0.012	
slc1Δ/slc1Δ in YPD		0.115	0.015	0.382
SLC1Δ/slc1Δ in YPD				0.669
BY4743 in F1	1.013	0.692	0.008	3.616
ino1Δ/ino1Δ in F1 - inositol		0.280	0.002	0.588
slc1Δ/slc1Δ in F1	0.279			1.187

The ultimate goal of the study was to determine the most appropriate region of the sphingolipid signaling cascade for the development of an efficient therapeutic agent for several important diseases like cancer. Since *ino1Δ/ino1Δ* and *ser2Δ/ser2Δ* mutants possessed elevated P-Cer and D-Cer levels with relatively low biomass values, these enzymes might be appropriate candidates of drug targets. Also, since *slc1Δ/slc1Δ* mutant showed a proliferating profile instead of an apoptotic one with elevated PHS and DHS levels as well as biomass values, overexpression of *SLC1* which encodes Slc1p catalyzing the production of PA might also be a good candidate for drug target.

5.2. Recommendations

Chemostat cultivations may be carried out instead of batch experiments, to have a better control on the cells during growth. To do chemostat experiments, a sampling method should be developed since 100 ml samples need to be collected for lipid extraction. Also different media having different inositol and serine concentrations may be used to better understand the effect of transport reactions.

For *ser2Δ/ser2Δ* mutant, F1 medium with varying serine concentrations could be adopted to make its growth possible in a medium other than YPD. All the heterozygous

mutant strains should be grown in F1 medium to observe the effect of initial concentrations of compounds present in the medium, such as inositol, ammonia, serine etc.

Several more genes may be investigated for their sphingolipid profiles, especially over expression mutants of different genes, such as *SLC1* and *INO1*. Hence, more accurate results may be obtained on the activity of the specific enzymes and on how the cell responded to them.

A convenient internal standard of known concentration may be used to count for the losses during the lipid extraction process so that the sphingolipid concentration values given by HPLC would be normalized accordingly. This internal standard must have a retention time value totally different than the sphingolipids in yeast, and must be detected by the mobile phase used for the detection of sphingolipids by HPLC. One last suggestion may be the use of suitable filters which would be used prior to the injection of samples to HPLC to avoid the noise present on the chromatograms.

APPENDIX A: CALIBRATION CURVES

A.1. Calibration Curve and Equation for C8-Cer

Various types of trend lines were tested and the best fitted trend line type was chosen according to the heighest R^2 value.

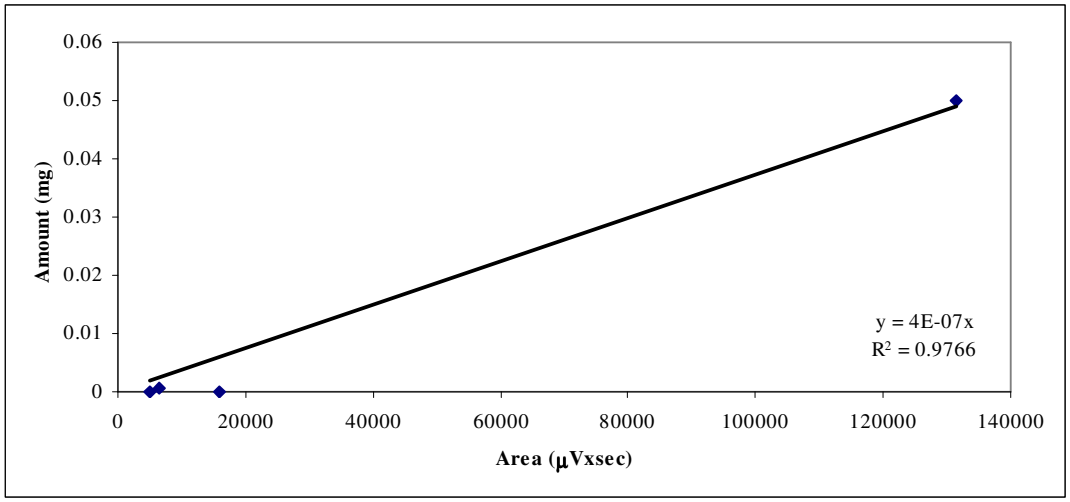

Figure A.1. Calibration curve for C8-Cer

From Figure A.1 , it is seen that the calibration curve constructed was a linear one. The x-axis showed the area in μV x sec, which is the product of height of the peak on the chromatogram in μV and time in sec. while the y-axis was the amount of injected C8-Cer in mg. The equation of this calibration curve was as follows:

$$y = 4 \times 10^{-7} x \qquad \text{(A.1)}$$

A.2. Calibration Curve and Equation for C6-Cer

As it is seen on Figure A.2, the calibration curve constructed was a second order polynomial one. The x-axis showed the area in μV x sec, while the y-axis was the amount of C6-Cer injected in mg. The equation of this calibration curve was as follows:

$$y = 2\times10^{-16}x^2 + 10^{-10}x \qquad \text{(A.2)}$$

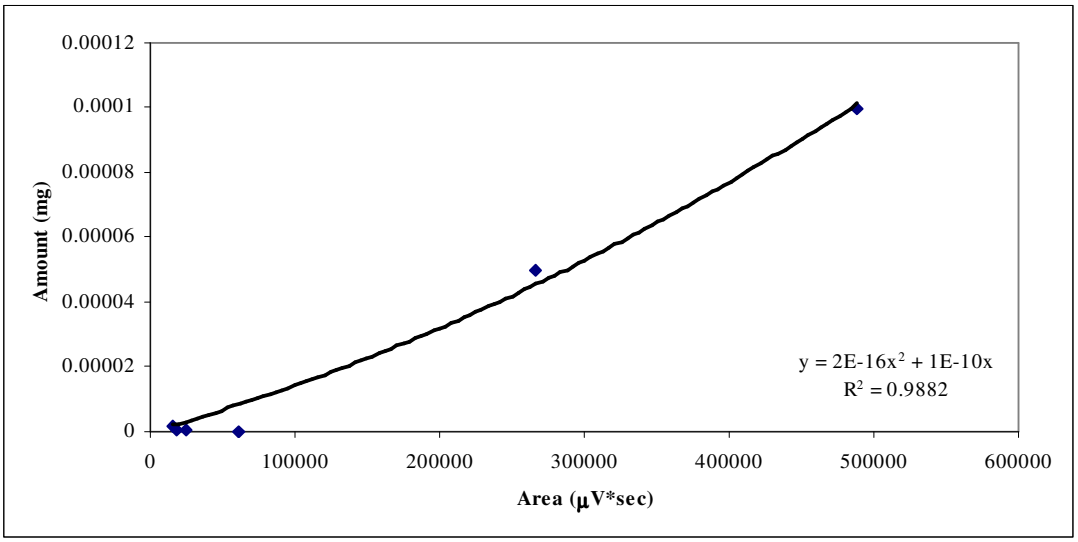

Figure A.2. Calibration curve for C6-Cer

A.3. Calibration Curve and Equation for C2-Cer

The calibration curve given on Figure A.3, was a second order polynomial one. The x-axis showed the area in µV x sec, which is the product of height of the peak on the chromatogram in µV and time in sec. while the y-axis was the amount of C2-Cer injected in mg.

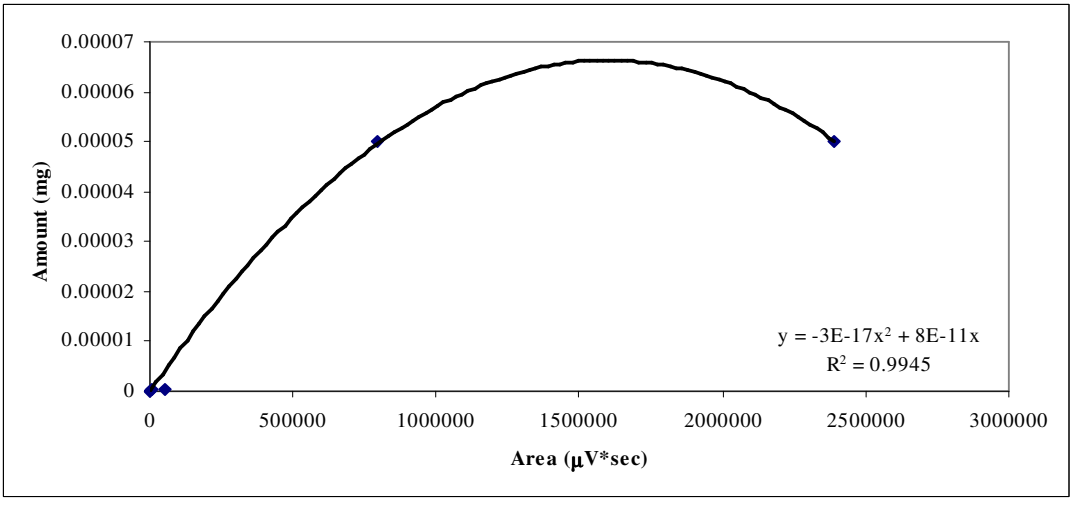

Figure A.3. Calibration curve for C2-Cer

The equation of this calibration curve was as follows:

$$y = -3\times10^{-17}x^2 + 8\times10^{-11}x \qquad \text{(A.3)}$$

A.4. Calibration Curve and Equation for P-Cer

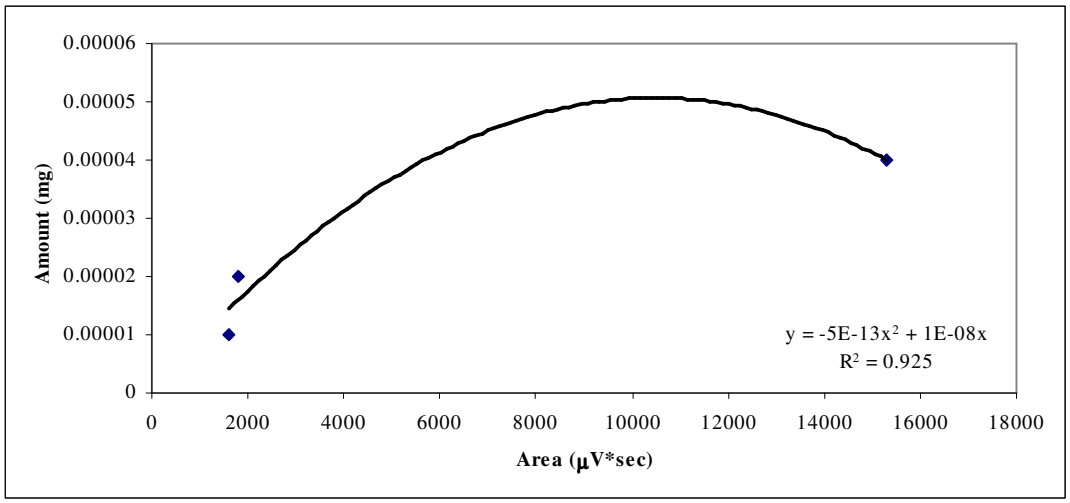

Figure A.4. Calibration curve for P-Cer

As can be seen from Figure A.4, the calibration curve constructed is a second order polynomial one. The x-axis shows the area in µV x sec, which is the product of height of the peak on the chromatogram in µV and time in sec. while the y-axis is the amount of P-Cer injected in mg. The equation of this calibration curve was as follows:

$$y = -5\times10^{-13}x^2 + 10^{-8}x \qquad \text{(A.4)}$$

A.5. Calibration Curve and Equation for PHS

As it is seen from Figure A.5, the calibration curve constructed is a second order polynomial one. The x-axis shows the area in µV x sec, which is the product of height of the peak on the chromatogram in µV and time in sec. while the y-axis is the amount of PHS injected in mg. The equation of this calibration curve is as follows:

$$y = -10^{-12}x^2 + 2\times10^{-8}x \qquad \text{(A.5)}$$

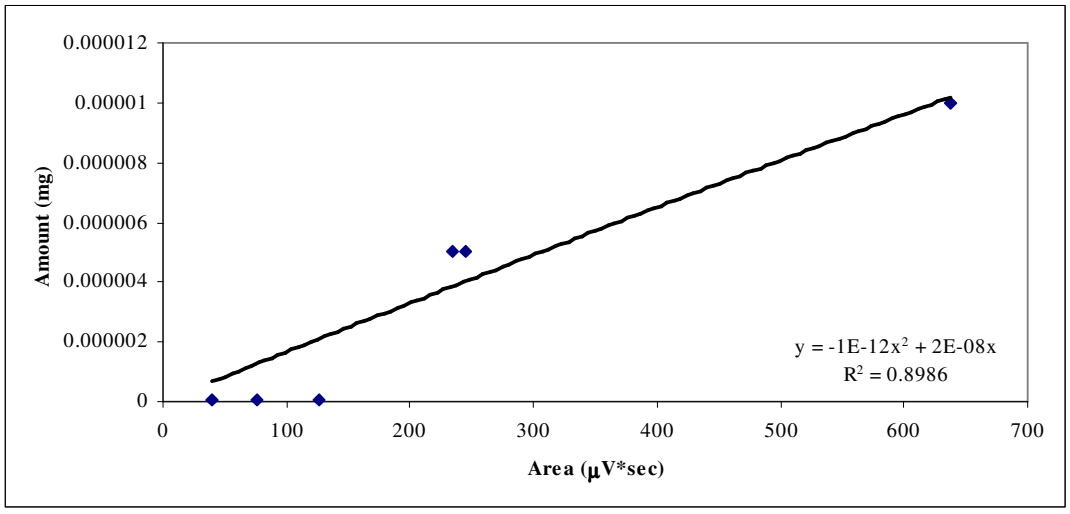

Figure A.5. Calibration curve for PHS

A.6. Calibration Curve and Equation for C18-DHS

Various types of trend lines were tested and the best fitted trend line type was chosen according to the heighest R^2 value.

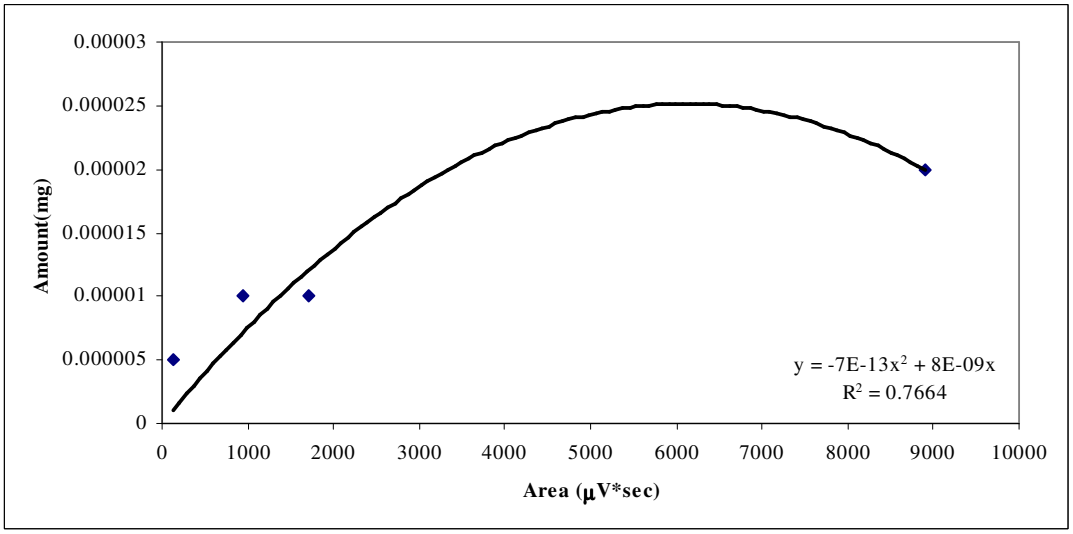

Figure A.6. Calibration curve for C18-DHS

As it is seen from Figure A.6, the calibration curve constructed is a second order polynomial one. The x-axis shows the area in μV x sec, which is the product of height of the peak on the chromatogram in μV and time in sec. while the y-axis is the amount of C18-DHS injected in mg. The equation of this calibration curve is as follows:

$$y = -7\times10^{-13}x^2 + 8\times10^{-9}x \qquad \text{(A.6)}$$

A.7. Calibration Curve and Equation for C20-DHS

Various types of trend lines were tested and the best fitted trend line type was chosen according to the heighest R^2 value.

From Figure A.7, it is seen that the calibration curve constructed is a second order polynomial one. The x-axis shows the area in μV x sec, which is the product of height of the peak on the chromatogram in μV and time in sec. while the y-axis is the amount of C20-DHS injected in mg. The equation of this calibration curve is as follows:

$$y = -8\times10^{-16}x^2 + 5\times10^{-10}x \qquad \text{(A.7)}$$

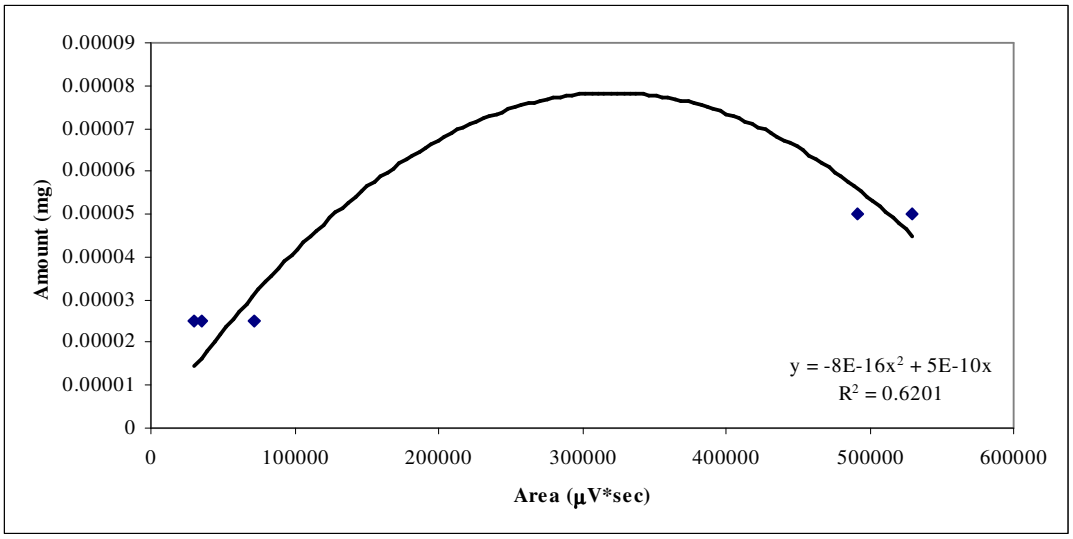

Figure A.7. Calibration curve for C20-DHS

REFERENCES

Albers E., V. Laizé, A. Blomberg, S. Hohmann and L. Gustafsson, 2003, "Ser3p (Yer081wp) and Ser33p (Yil074cp) are Phosphoglycerate Dehydrogenases in *Saccharomyces cerevisiae*", *Journal of Biological Chemistry*, Vol. 278, pp. 10264-10272.

Alvarez-Vasquez F. , K. J. Sims, L. A. Cowart, Y. Okamoto, E. O. Voit and Y. A. Hannun, 2005, "Simulation and Validation of Modelled Sphingolipid Metabolism in *Saccharomyces cerevisiae*", *Nature*, Vol. 433, pp. 425-430.

Athenstaedt K. and G. Daum, 1997, "Biosynthesis of Phosphatidic Acid in Lipid Particles and Endoplasmic Reticulum of *Saccharomyces cerevisiae*", *Journal of Bacteriology*, Vol. 179**,** pp. 7611- 7616.

Athenstaedt K. and G. Daum, 1999, "Phosphatidic Acid , a Key Intermediate in Lipid Metabolism", *European Journal of Biochemistry*, Vol. 266, pp. 1-16.

Belhumeur P. , N. Fortin and M. W. Clark, 1994, "A Gene from *Saccharomyces cerevisiae* Which Codes for a Protein With Significant Homology to the Bacterial 3-Phosphoserine Amino Transferase", *Yeast*, Vol. 10, pp. 385-389.

Benghezal M. , C. Roubaty, V. Veepuri, J. Knudsen and A. Conzelmann, accepted, "*SLC1* and *SLC4* Encode Partially Redundant Acyl-Coenzyme A 1-acylglycerol-3-Phosphate Oacyltransferases of Budding Yeast", *Journal of Biological Chemistry*.

Birbes H. , S. El Bawab, Y. A. Hannun and L.M. Obeid, 2001, "Selective Hydrolysis of a Mitochondrial Pool of Sphingomyelin Induces Apoptosis", *FASEB Journal*, Vol. 15, pp. 2669–2679.

Bligh E. G. and W. J. Dyer, 1959, "A Rapid Method for Total Lipid Extraction and Purification", *Canadian Journal of Biochemical Physiology*, Vol. 37, pp. 911-917.

Buede R. , C. Rinker-Schaffer, W. J. Pinto, R. L. Lester and R. C. Dickson, 1991, "Cloning and Characterization of LCB1, a Saccharomyces Gene Required for Biosynthesis of the Long-chain Base Component of Sphingolipids", *Journal of Bacteriology*, Vol. 173, pp. 4325-4332.

Chung N. , C. Mao, J. Heitman, Y. A. Hannun and L. M. Obeid, 2001, "Phytoshingosine as a Specific Inhibitor of Growth and Nutrient Import in *Saccharomyces cerevisiae*" *The Journal of Biological Chemistry*, Vol. 276, pp. 35614-35621.

Colombaionia L. and M. Garcia-Gil, 2004, "Sphingolipid Metabolites in Neural Signalling and Function", *Brain Research Reviews*, Vol. 46, pp. 328–355.

David D. , S. Sundarababu and J. E.Gerst, 1998, "Involvement of Long Chain Fatty Acid Elongation in the Trafficking of Secretory Vesicles in Yeast", *Journal of Cell Biology*, Vol. 143, pp. 1167-1182.

Dean-Johnson M. and S. A. Henry, 1989, "Biosynthesis of Inositol in Yeast: Primary Structure of Myo-inositol-1-phosphate Synthase (EC 5.5.1.4) and Functional Analysis of its Structural Gene, the INO1 Locus", *Journal of Biological Chemistry*, Vol. 264, pp. 1274-1283.

Dickson R. C. , G. B. Wells, A. Schmidt and R. L. Lester, 1990, "Isolation of Mutant *Saccharomyces cerevisiae* Strains that Survive Without Spingolipids", Molecular Cell Biology, Vol. 10, pp. 2176–2181.

Dickson R. C. and R. L. Lester, 1999a, "Metabolism and Selected Functions of Sphingolipids in the Yeast *Saccharomyces cerevisiae*", *Biochimica et Biophysica Acta*, Vol. 1438, pp. 305-321.

Dickson R. C. and R. L. Lester, 1999b, "Yeast Sphingolipids", *Biochimica et Biophysica Acta*, Vol. 1426, pp. 347-357.

Fahy E. , S. Subramaniam, H. A. Brown, C. K. Glass, A. H. Merrill, Jr., R. C. Murphy, C. R. H. Raetz, D. W. Russell, Y. Seyama, W. Shaw, T. Shimizu, F. Spener, G. van Meer, M. S. VanNieuwenhze, S. H. White, J. L. Witztum and E. A. Dennis, 2005, "A Comprehensive Classification System for Lipids", *Journal of Lipid Research*, Vol. 46, pp. 839-862.

Fishbein J. D. , R. T. Dobrowsky, A. Bielawska, S. Garrett and Y. A. Hannun, 1993, "Ceramide Mediated Growth Inhibition and CAPP are Conserved in *Saccharomyces cerevisiae*", *Journal of Biological Chemistry*, Vol. 268, pp. 9255-9261.

Gable K. , G. Han, E. Monaghan, D. Bacikova, M. Natarajan, R. Williams and T. M. Dunn, 2002, "Mutations in the Yeast *LCB1* and *LCB2* Genes, Including Those Corresponding to the Hereditary Sensory Neuropathy Type I Mutations, Dominantly Inactivate Serine Palmitoyltransferase", *The Journal of Biological Chemistry*, Vol. 277, pp. 10194-10200.

Greenberg M. L. and J. M. Lopes, 1996, **"**Genetic Regulation of Phospholipid Biosynthesis in *Saccharomyces cerevisiae*", *Microbiol Reviews*, Vol. 60, pp. 1-20.

Griac P. and S. A. Henry, 1999, "The Yeast Inositol-sensitive Upstream Activating Sequence, UASINO, Responds to Nitrogen Availability", *Nucleic Acids Research*, Vol. 27, pp. 2043-2050.

Hannun Y. A. , C. R. Loomis, A. H. Merrill, R. M. Bell, 1986, "Sphingosine Inhibition of Protein Kinase C Activity and of Phorbol Dibutyrate Binding in vitro and in Human Platelets", *Journal of Biological Chemistry*, Vol. 261, pp. 12604–12609.

Irie F. and Y. Hirabayashi, 1998, "Application of Exogenous Ceramide to Cultured Rat Spinal Motoneurons Promotes Survival or Death by Regulation of Apoptosis Depending on its Concentrations", *Journal of Neuroscience*, Vol. 54, pp. 475-485.

Jenkins G. M. and Y. A. Hannun, 2001, "Role for de novo Sphingoid Base Biosynthesis in the Heat-induced Transient Cell Cycle Arrest of *Saccharomyces cerevisiae*", *Journal*

of Bioogical Chemistry, Vol. 276, pp. 8574-8581.

Kavun B. and K. Ülgen, 2005, "Metabolic Control Analysis and Metabolic Pathway analysis of Sphingolipid Metabolism for Anticancer Drug Target Identification", *12th European Congress on Biotechnology*, İstanbul, 21 August-24 August 2005, Copenhagen, Denmark.

Kihara A. and Y. Igarashi, 2004, "FVT-1 Is a Mammalian 3-Ketodihydrosphingosine Reductase With an Active Site That Faces the Cytosolic Side of the Endoplasmic Reticulum Membrane", *Journal of Biological Chemistry*, Vol. 279, pp. 49243-49250.

Kolesnick R. N, 1987, "1,2-Diacylglycerols but not Phorbol Esters Stimulate Sphingomyelin Hydrolysis in GH3 Pituitary Cells", *Journal of Biological Chemistry*, Vol. 262, pp. 16759–16762.

Lopes J. M. , J. P. Hirsch, P. A. Chorgo, K. L. Schulze, and S. A. Henry, 1991, "Analysis of Sequences in the INO1 Promoter that are Involved in its Regulation by Phospholipid Precursors", *Nucleic Acids Research*, Vol. 19, pp. 1687-1693.

Mandon E. C. , G. van Echten, R. Birk, R. R. Schmidt and K. Sandhoff, 1991, "Sphingolipid Biosynthesis in Cultured Neurons: Down Regulation of Serine Palmitoyl Transferase by Sphingoid Bases", *European Journal of Biochemistry*, Vol. 198, pp. 667-674.

McNabb T. J. , A. E. Cremesti, P. R. Brown and A. S. Fischl, 1999, "The Separation and Direct Detection of Ceramides and Sphingoid Bases by Normal-phase High-performance Liquid Chromatography and Evaporative Light-scattering Detection", *Analytical Biochemistry*, Vol. 276, pp. 242-250.

Merrill A. H. , A. M. Sereni, V. L. Stevens, Y. A. Hannun, R. M. Bell and J. M. Kinkade, 1986, "Inhibition of Phorbol Ester-dependent Differentiation of Human Promyelocytic Leukemic (HL-60) Cells by Sphinganine and Other Long-chain Bases", *Journal of Biological Chemistry*, Vol. 261, pp. 12610–12615.

Merrill A. H. and C. C. Sweeley, 1996, "*Biochemistry of Lipids, Lipoproteins and Membranes*", Third Edition, Elsevier Science, New York.

Merrill A. H. , Jr. , M. C. Sullards , J. C. Allegood, S. Kelly and E. Wang, 2005, "Sphingolipidomics: High-throughput, Structure-specific, and Quantitative Analysis of Sphingolipids by Liquid Chromatography Tandem Mass Spectrometry", *Methods*, Vol. 36, pp. 235–245.

Nagiec M. M. , G. B. Wells, R. L. Lester and R. C. Dickson, 1993, "A Suppressor Gene that Enables *Saccharomyces cerevisiae* to Grow Without Making Sphingolipids Encodes a Protein that Resembles an *Escherichia coli* Fatty Acyltransferase", *Journal of Biological Chemistry*, Vol. 268, pp. 22156-22163.

Nagiec M. M. , J. A. Baltisberger, G. B. Wells, R. L. Lester and R. C. Dickson, 1994, "The LCB2 Gene of Saccharomyces and the Related LCBJ Gene Encode Subunits of Serine Palmitoyltransferase, the Initial Enzyme in Sphingolipid Synthesis", *Biochemistry*, Vol. 91, pp. 7899-7902.

Nagiec M. M. , E. E. Nagiec, J. A. Baltisberger, G. B. Wells, R. L. Lester and R.C. Dickson, 1997, "Sphingolipid Synthesis as a Target for Antifungal Drugs Complementation of the Inositol Phosphorylceramide Synthase Defect in a Mutant Strain of *Saccharomyces cerevisiae* by the *Aur1* Gene", *Journal of Biological Chemistry*, Vol. 272, pp. 9809-9817.

Nickels J. T. and J. R. Broach, 1996, "A Ceramide-activated Protein Phosphatase Mediates Ceramide-induced G1 Arrest of *Saccharomyces cerevisiae*", *Genes and Development*, Vol. 10, pp. 382-394.

Obeid L. M. , Y. Okamoto, C. Mao, 2002, "Yeast Sphingolipids: Metabolism and Biology", *Biochimica et Biophysica Acta*, Vol. 1585, pp. 163-171.

Puoti A. , C. Desponds and A. Conzelmann, 1991, "Biosynthesis of Mannosylinositol Phosphoceramide in *Saccharomyces cerevisiae* is Dependent on Genes Controlling

the Flow of Secretory Vesicles from the Endoplasmic Reticulum to the Golgi", *Journal of Cell Biology*, Vol. 113, pp. 515-525.

Qie L. X., M. M. Nagiec, J. A. Baltisberger, R. L. Lester and R. C. Dickson, 1997, "Identification of a *Saccharomyces* Gene, *LCB3*, Necessary for Incorporation of Exogenous Long Chain Bases into Sphingolipids", *Journal of Biological Chemistry*, Vol. 272, pp. 16110–16117.

Reynolds C. P. , B. J. Maurera and R. N. Kolesnick, 2004, "Ceramide Synthesis and Metabolism as a Target for Cancer Therapy", Cancer letters, Vol. 206, pp. 169-180.

Salinas M. , R. Lopez-Valdaliso, D. Martin, A. Alvarez and A. Cuadrado, 2000, "Inhibition of PKB/Akt1 by C2-ceramide Involves Activation of Ceramide-activated Protein Phosphatase in PC12 Cells", *Molecular and Cellular Neuroscience*, Vol. 15, pp. 156-169.

Shirra M. K. and K. M. Arndt, 1999**,** "Evidence for the Involvement of the Glc7-Reg1 Phosphatase and the Snf1-Snf4 Kinase in the Regulation of INO1 Transcription in *Saccharomyces cerevisiae*", *Genetics*, Vol. 152, pp. 73-87.

Smith S. W. and R. L. Lester, 1974, "Inositolphosphorylceramide, a Novel Substance and the Chief Member of a Major Group of Yeast Sphingolipids Containing a Single Inositol Phosphate", *Journal of Biological Chemistry*, Vol. 249, pp. 3395-3405.

Spiegel S. and S. Milstien, 2003, "Sphingosine-1-phosphate: an Enigmatic Signalling Lipid", *Nature Reviews Molecular Cell Biology*, Vol. 4, pp. 397–407.

Spiegel S. , D. Foster and R. N. Kolesnick, 2003, "Signal Transduction Through Lipid Second Messengers", *Current Opinion in Cell Biology*, Vol. 8, pp. 159–167.

Verheij M. , R. Bose, X. H. Lin, B. Yao, W. D. Jarvis, S. Grant, M. J. Birrer, E. Szabo, L. I. Zon, J. M. Kyriakis, A. Haimovitz-Friedman, Z. Fuks and R. N. Kolesnick, 1996,

"Requirement for Ceramide-initiated SAPK/JNK Signalling in Stress-induced Apoptosis", *Nature*, Vol. 380, pp. 75-79.

Wells G. B. , R. C. Dickson and R. L. Lester, 1998, "Heat-induced Elevation of Ceramide in *Saccharomyces cerevisiae* Via de novo Synthesis", *Journal of Biological Chemistry*, Vol. 273, pp. 7235-7243.